RESPONSE TO REVIEWERS:

We are grateful to both reviewers for the many insightful and constructive comments, in addition to the suggestions on process descriptions that have clearly strengthened the study. Our responses (in black) to the issues raised (red) are presented below.

REVIEWER 1

Major Comments

The structure of the results section could be improved. First, it would be better if there were a comparison of a control simulation with observations (model validation). The control run should be the most realistic of the simulations that the authors can manage, which would be expected to include breakup. Second, once the control run is validated, then the sensitivity tests should be shown, excluding the various processes.

Good point. The CNTRL LES simulation is now the one that include all SIP mechanisms and we have attempted to evaluate the validity of the simulations to the fullest extent possible with the observational data available.

Also the description of the simulations with various IN assumptions is vague, with the temperature of each active IN concentration being not mentioned.

In the original submission we prescribed a constant INP concentration throughout the domain, which corresponds to the mean primary ice concentration estimated offline with DeMott parameterization (averaged over the observed temperature range). In the revised manuscript we have implemented the aerosol-aware DeMott parameterization in the LES to allow for INP to respond to aerosol concentration and temperature. What is interesting is that despite this adjustment, the LES dynamics tends to mix the INP throughout the cloudy column, so that a quasi-homogeneous INP profile still emerges (see Figure S1 in the revised Supporting Information)

Also, it is a struggle to reconcile the model with observations in Fig. 9b. One or two simulations without breakup seem more accurate than those with breakup. Yet in the abstract you write the inclusion of breakup brings the model into agreement with observations for the case.

In Fig 9b in the initial manuscript the only simulation without break-up that gives a better representation of the number concentrations is IN1; this is because an extremely high initial INP concentration ~ 1 L^{-1} is prescribed (see Figure 1 below). However, even when we activate SIP in these unrealistic conditions (INP1_SIP) the mean concentration goes up to 2-3 L^{-1}, without affecting the ice water mixing ratio. In all other cases (IN0.01_SIP and ALLSIP) activating BR improves the results, as the produced concentrations fall within the observed range. For this reason we state that including BR in the microphysics scheme is likely required to reconcile the simulations with observations. Note that in the revised manuscript, all relevant results are updated with the INP predicted by the DeMott INP parameterization – and the conclusion still remains unchanged.

Detailed Comments

Abstract

The term "droplet-shattering" is used where I think it would be more accurate to say "drop shattering" or "rain/drizzle-drop shattering". The type of shattering that the authors refer to is of drops > 0.05 mm in diameter, while cloud-droplets are typically smaller than this. Cloud-

droplets are < 0.05 mm diameter and are observed not to shatter or splinter.
Indeed so. The term is now changed to "drop-shattering"

1. Introduction
Line 168: I thought Savre had developed an ice nucleation scheme with the MISU group. So I wonder why it is not being applied here.
MIMICA can conduct simulations with the Phillips nucleation schemes (Phillips et al. 2013) and a scheme based on Classical Nucleation Theory (Savre and Ekman 2015). Both however require knowledge of the aerosol composition of the studied atmospheric conditions (number of mineral dust, organic, BC particles), but such measurements are not available during ACCACIA. Nevertheless, to explicitly simulate the heterogeneous ice nucleation process, we have now implemented in MIMICA the DeMott parameterization with mean aerosol measurements from ACCACIA as input.

2. ACCACCIA
Page 4, "between 10-11 UTC" should be "between 10:00 and 11:00 UTC".
Thank you, corrected.

3. Models and Methods
It is written "Ice nucleation is also parameterized following Morrison et al. (2011): ICNCs fall below the prescribed INP concentration (NINP), they are nudged upward towards the INP value. " But this seems less accurate than tracking the number concentration of IN lost by activation with a separate prognostic variable, as pioneered by Cohard and Pinty in the 1990s. Computational cost would be minimal. To avoid confusion, it would be a good idea to paraphrase that the "active IN concentration" (I prefer this phrase over "INP" concentration since it is self-evident that the IN is a particle and what is important is the activity spectrum; there is no single number for the concentration) is prescribed from the DeMott 2010 parameterisation informed by total aerosol measurements of the ACCACIA case.
The points raised by the reviewer are well taken. Including INP as a prognostic variable (thus explicitly describe both nucleation and INP recycling processes) is something that requires significant development, and therefore beyond the scope of this manuscript. However, the temperature-dependent aerosol-aware nucleation scheme by DeMott is now directly implemented in the LES. To avoid continuous nucleation with time and excessive production of primary production of ice crystals, we limit activation with the same method as it is done in the standard Morrison scheme in WRF: new nucleated particles = INP (as estimated by DeMott) - existing N_{ice}. If this is negative, then no nucleation is assumed to occur. This is a simplified way to account for INPs lost by activation in previous timesteps and can be found in standard microphysics schemes, such as Morrison et al. (2005)

The DeMott scheme has no dependence on aerosol chemical composition and size. The scheme implicitly assumes that only dust is the IN species, since concentrations in the measurements setting up the DeMott scheme originally involved dust dominating the sizes > 0.5 micron. How does one know that bio-IN were not dominating the IN activity in this case? Or soot from biomass-burning? One wonders if another scheme with aerosol chemistry/size dependencies might be more accurate. A sensitivity test with respect to choice of IN scheme would be a good idea.
The DeMott scheme is definitely not as advanced as any other aerosol-chemistry-aware scheme. However, it has been found to perform better in polar conditions than any other temperature-dependent scheme (e.g. Young et al. 2016, Listowski and Lachlan-Cope 2017), so it is considered the best option for cases where aerosol composition information is limited (as in our case). Interestingly enough, when mean aerosol measurements are used as input for -6.5^{o}C (the coldest simulated temperatures) this scheme predicts INP=0.03 L^{-1}, which is very close to the upper limit of INPs in

Wex et al. (2019) (Figure 1) that include the effect of bioaerosols. Even if the predicted INP concentration of 0.03 L^{-1} is likely realistic (Figure 1), when prescribed in the LES simulations, it does not produce substantial ice. For this reason we have to consider the uncertainty in the DeMott parameterization which is a factor of 10. But multiplying DeMott by a factor of 10 yields very large INP concentrations (~0.3 L^{-1}) near cloud top (minimum -6.5°C), which is unrealistic for warm subzero temperatures (Figure 1). For this reason, in our CNTRL simulation we multiply DeMott by a factor of 5, which gives INP concentrations that vary from 0.007 L^{-1} at cloud base (~ -3°C) to 0.11 L^{-1} near cloud top. However, the sensitivity to the assumed INP conditions is shown in the revised text with three additional tests: (a) original DeMott parameterization, (b) DeMott × 10 and (c) DeMott × 100

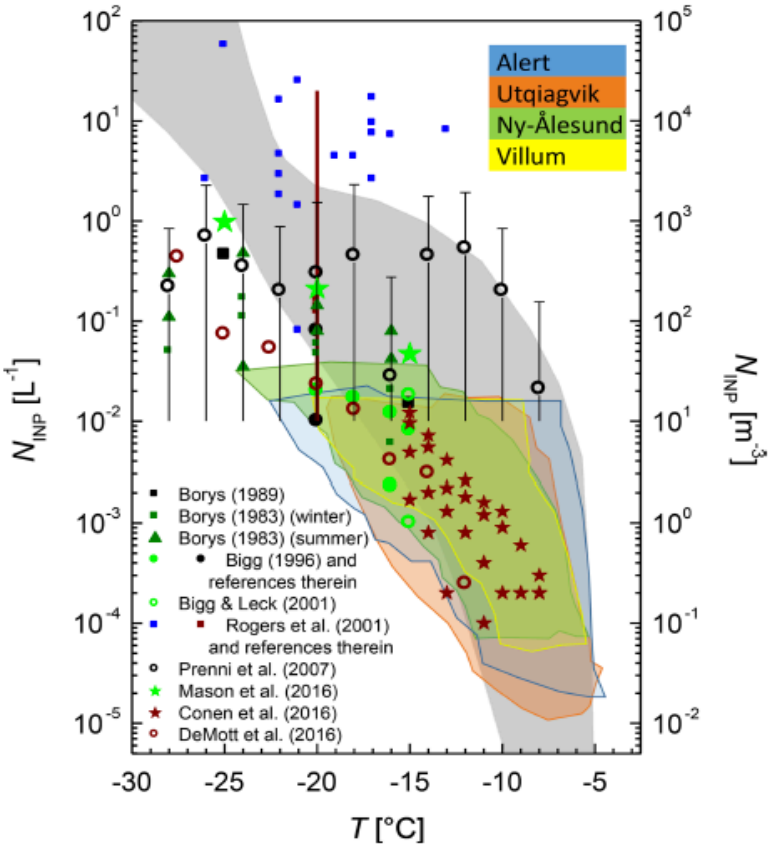

Figure 1: INP measurements conducted by Wex et al. (2019) at four Arctic sites: blue, red, green and yellow shaded areas represent Alert, Utqiagvik, Ny-Alesund and Villum, respectively. Literature data is also included by Petters and Wright (2015) (gray background), Borys (1983, 1989), Bigg (1996), Bigg and Leck (2001), Rogers et al. (2001), Prenni et al. (2007), Mason et al. (2016), Conen et al. (2016), and DeMott et al. (2016). Green and brown symbols represent data from surface-based measurements; black and blue represent airborne measurements. For Rogers et al. (2001), brown indicates data they cited from the literature, with the vertical bar indicating the extent of the reported values.

There must have been IN measurements in the Arctic in different years, so it would be best to include in the paper a plot of the active IN vs temperature comparing your scheme with the IN measurements from other Arctic campaigns in summertime of various years.

The most comprehensive Arctic measurements of IN have been recently documented in Wex et el. (2019). The paper includes relatively long-term measurements at four different Arctic sites for all seasons. They also include several Arctic INP datasets from the literature (see Figure 1 above), thus they give a very clear view of the limited concentrations in this region. Since this paper has very recently been published in ACP, we prefer to refer all readers to this very informative paper.

The breakup scheme is based on Takahashi 1995. But they observed collisions between two giant ice spheres (2 cm), one of which was rimed. Phillips et al. (2017a) when building their breakup scheme interpreted these as representing graupel-graupel collisions because the bulk density of the colliding spheres was that of pure ice, not graupel-snow collisions. Can the author comment on this ? Have the authors rescaled the Takahashi data to account for the typical sizes of the graupel in Arctic clouds.

Thank you for this suggestion, we had not scaled Takahashi results with size in the initial submission. Considering that Takahashi used cm-size particles, the overestimation in the number of fragments ejected from the collided particle surfaces in our model can vary from one to two orders of magnitude for μm or mm size ice crystals, respectively. For this reason, we conduct a series of sensitivity tests with the LPM in which Takahashi's relationship is reduced by a factor of: (a) 10, (b) 50 and (c) 100. The number of fragments predicted by these parameterizations is given in Figure 4 in the revised manuscript, while the LES results are shown in Figures 5-6. The original formula used in the original submission predicts more than 100 collisions in the temperature range of interest (Figure 4), which is likely a significant overestimation in SIP production.

The breakup scheme by Phillips et al. (2017a) is based realistically on collision kinetic energy and temperature, with different treatments for each permutation of species of collisions (graupel-graupel, graupel-snow, snow-snow) etc. It would be better for the authors to upgrade their treatment of breakup.

The point is well taken. Phillips et al. (2017a) requires several parameters that are not directly available by the model, including collision type, ice habit, rimed fraction of the particle that undergoes fragmentation. For each an assumption is made: *i*) as primary ice particles grow through vapor deposition and move to the second bin, we assume that this bin represents snow; *ii*) given the relatively warm temperature range (Pruppacher and Klett, 1997) and after inspection of particle images, planar ice is likely the most representative ice habit of ACCACIA conditions; *iii*) a rimed fraction of 0.4 is assumed, as lower values do not yield any SIP (because the fragments per collision become less than unity) and ice crystal number is highly underestimated. Finally, *iv*) the third LPM bin is assumed to consist of sufficiently rimed particles, thus the collision type adapted in our simulation is that of snow-graupel.

Since Phillips et al. (2017a) is the state-of-the art parameterization, we consider the LES run with this scheme to be the CNTRL simulation, while the more simplified temperature-dependent parameterizations are presented as sensitivity tests.

Finally, at this point we would like to highlight another modification in our LPM set-up in the revised manuscript. In the initial submission, LPM simulations were run either for 30 minutes or until the LPM temperature reaches -6.5°C which is the minimum cloud-top temperature simulated by the LES. The cloud mixing timescale τ_{mix} was set to 30 minutes, considering

$$\tau_{mix} = \frac{cloud\ depth}{mean\ updraft\ velocity}$$

However inspection of the LPM simulations with a mean updraft velocity of 0.25m s^{-1} and cloud-base temperature = -3.5°C revealed that cloud temperature drops to -5.5°C within 30 minutes; to reach the minimum LES temperature, another ~14 minutes of simulation are required. Hence, we run all LPM simulations for an hour instead, and let the cloud-top temperature threshold determine the actual length of each simulation.

The authors write "The mean observed INP concentration is 0.006 L-1 and never exceeds 0.05 L-1, while the mean and maximum observed ICNC for the same period is 1.43 L-1 and 17.8 L-1, respectively, suggesting substantial ice multiplication. " But the authors need to say what conditions of temperature and humidity are used to define these active IN concentrations.

These statistics are based on all the flight data collected on 23 July 2013,between 10:00 and 11:00 UTC, at a range of latitudes, longtitudes and altitudes. They aim to provide a more general overview and also allow for comparison with other ACCACIA flights (e.g. Lloyd et al. 2015) in which INP conditions are estimated and presented in a similar way. In retrospect, we see that this discussion may

be too vague, and is now clarified: $0.006L^{-1}$ is the mean concentration is for the whole flight, which sampled at temperatures between ~ -10 °C – 0 °C and specific humidity ~ 2.5–5 g m^{-3}. The maximum INP concentration is observed at ~ T= -10 °C and Qv=2.5 g m^{-3}. The maximum ICNC occurs at T~-5°C, much warmer conditions than those that maximum INPs are measured, suggesting that SIP may be occurring.

4. Results

The conclusion stated in the Abstract is plausible: "In contrast, break-up enhances ICNCs by 1-1.5 orders of magnitude, bringing simulations in good agreement with observations". However inspection of Fig. 9b comparing predicted and observed ice concentrations shows that the control run without ice multiplication is an order of magnitude too low and with it is an order of magnitude too high.

We have now addressed this in the revised manuscript (after scaling Takahashi's results and also testing Phillip's parameterization; see Figure 5 in the revised version).

It seems confusing that the run without ice multiplication is referred to as the "control" and is depicted with a dashed line rather than a full line.

Sorry for that, in the revised version CNTRL simulation is always represented with a full line.

I wonder if the over-prediction of breakup is due to inaccuracy in the formula. Were the Takahashi observations re-scaled for the smaller particles relative to the lab experiment? Takahashi did when he applied his own lab data to provide estimates for natural clouds.

The revised manuscript now considers three different scaling factors to the Takahashi data; these are presented as sensitivity tests along with the control simulation, which employs Phillips parameterization (Figures 5-6 in the revised manuscript). The scaling factor Fbr/100 is more accurate for particles~ 100μm. The scaling factor Fbr/50 is more representative for particles~500 μm and Fbr/10 corresponds to mm sizes, considering that Takahashi et al. (1995) used cm-sized hailballs in their experiments.

5. Discussion

The paper by Schwarzenboeck et al. (2009) was seminal and totally relevant as a motivation for the present study. So, there needs to be a more thorough description of their analysis and how they arrived at their estimate of about half (20-80%) of all ice particles being naturally fragmented. They were aware of the shattering bias issue quantified by Field et al. and Korolev et al., and did a diligent study. A few more sentences describing the paper are needed.

The findings of Schwarzenboeck et al. (2009) are now more extensively discussed in the last section of the revised manuscirpt.

Line 449: The comment about the fallout time-scale not being objectively defined could be misinterpreted. What the authors intend to say is that in their own model, the fall-out time-scale can have values in a wide range (there is a similar timescale parameter in the Yano-Phillips theory).

This discussion is now removed to avoid any misinterpretation. This paragraph discussed uncertainties in τ_g which is the timescale for medium ice particles (2^{nd} bin) to grow to large graupels. However, your comment suggests that the readers get the impression that this parameter can have values in a wide range, but this is not the case with our simulations. In Yano and Phillips (2011) τ_g is set 30 min, which was considered an upper limit for deeper convective clouds. In a shallow Arctic stratocumulus layer 30 min can sometimes be the timescale mixing for the whole cloud. Given that ice particles with a diameter ~400 m are found 130 m above cloud base and more systematically 260 m above this level

(Figure S2 in the revised Supporting Information) in the observations, the τ_g in our conditions is shorter than in their study. The adapted timescale 17.5 min is a reasonable approximation, estimated straight from the observations using the mean LES updraft velocity.

An order of magnitude estimate of the 'multiplication efficiency' (tilde c) for breakup in the model would be helpful, using the formula for it from Yano and Phillips (2011). Al though their theory was originally for graupel-graupel collisions, Phillips et al. (2017b) argued it also applies to graupel-snow collisions with a few changes of the parameters. The multiplication efficiency then implies a time-scale for the growth of ice concentration. Does the simulated time-scale of the explosion match the modified theory?

$\hat{C} = 4C_o$ ã τ_g $\tau_{G,}$ where C_o is the nucleation rate and ã= αN, where α is the sweep-out rate and N is the break-up rate. In our case the nucleation rate is estimated about ~ 0.02 s^{-1} m^{-3} , which is calculated as the product of updraft velocity, an assumed lapse rate of 6 K km^{-1}, and the temperature derivative of the INP concentration estimated with DeMott × 5 parameterization. Phillips and Takahashi's parameterization scaled with a factor 50-100 predict less than 5 fragments per collision in the temperature range of interest (Figure 4 in the revised version). Thus we use the upper limit N=5 in our calculations of the multiplication efficiency. α is set to 2.4×10^{-5} m^3 s^{-1}, adapted from Yano and Phillips (2011). Substituting these values in the above equation yields $\hat{C}$ = 10.58, which is in excellent agreement with the value $\hat{C}$ = 10 cited in Phillips et al. (2017b). This discussion is also added in Section 4.2 in the revised manuscript.

Does the theory predict that the Arctic clouds simulated is in the unstable regime of the phase-space ?

This is an excellent question. While $\hat{C}$ >1, which allows the potential explosive multiplication at some point, the limited timescale allowed for SIP to develop is the ultimate limiting factor in Arctic stratocumulus. The theory suggests that over a time scale of an hour, the multiplication is a factor of 10. Given that 60 min is an upper limit for cloud mixing timescale in in these shallow cloud layers, we don't expect ice multiplication to substantially overcome this factor. That said, being in the unstable regime is a requirement for SIP to provide crystals above the primary nucleated concentration.

REVIEWER 2:

What is the role of measurement conditions? It is said that the wind is from the West and measurements are performed both over the open water and ice. Droplet concentration seems similar in both, but there is no discussion how ice particle concentration differs and where the presented values are measured.

An overview of the observed conditions with respect to ice-covered or open-water surface was provided in Jones et al (2018). However since this manuscript remained in the discussion phase, a brief recap on the influence of the surface state on cloud microphysical properties is now added (lines 331-335 in the revised version). In the initial submission, in lines 271-273 we state that we use cloud measurements collected at latitudes higher than 81.7°N and within a 9×33 km^2 ice-covered area to evaluate the simulated cloud properties, as ice-covered surface conditions are also prescribed in the LES. Thus all cloud observations shown in Figures 5-7-9 in the initial document are collected over ice.

Is there any potential for the surface to be the source if ice hydrometeors?

Blowing snow is associated with strong winds over flat terrain (e.g. Vali et al. 2012; Gossart et al. 2017) or close to mountainous slopes in the vicinity of orographic clouds (e.g. Lloyd et al. 2015; Geerts et al 2015). A general threshold in 2-m wind speed for such events in freshly fallen snow is 7–10 m s^{-1}, with a weak trend toward lower threshold speeds at lower air temperatures (Dery and Yau

1999). Gossart et al. (2017) showed that the height of the blowing snow layer is usually << 500 m, except for stormy cases of heavy mixed events, precipitation and blowing snow ,when it can go up to 1.3 km. In our case, the winds are much weaker, on average ~ 5.8 m s^{-1} and the cloud base height is >500 m AGL, while the largest concentrations were observed at ~800 m AGL. A maximum height of 500 m for such phenomena is also recorded in Geerts et al (2017), but required much higher winds than in our case. Thus we believe there is no possibility for blowing snow to impact the examined clouds (this is also mentioned at the end of section 2.2 in the revised text) .

2) LPM: I have some problems in understanding what the LPM model employed is actually simulating. Does it solve the hydrometeor condensational growth assuming three size classes both for liquid and ice, or is it somehow parameterized how particles grow from some size range to another based on characteristic time parcel is spending in a single updraft. I'm actually surprised that there is no spectral size resolving model employed. Such models should be available and numerically efficient enough to be used in the presented application. In line 139 it is stated "The LPM allows a detailed description of the formation, growth and evolution of cloud droplets and ice particles as they interact with each other". I disagree with this, I would not call three bins detailed what comes to representation of cloud and ice particle size distributions. Thus also coagulation rate and secondary ice production are only approximate, although probably accurate enough to provide first estimates and to be used in this paper.

The LPM allows all bins to evolve dynamically by predicting their size as a function of temperature and supersaturation. However the transition from one bin to another is controlled by the timescales. This is based on Yano and Phillips (2011) and is a simple but still convenient framework to parameterize SIP. While more advanced spectral size resolving models would likely offer more accurate predictions of SIP effects, these are computationally expensive and do not allow SIP investigations over a very large parameter space. Here we demonstrate the possibility of using a simplified framework to develop parcel-model based parameterizations for larger scale models. However, we agree that this is not a very detailed model, and we have replaced the word 'detailed' with 'adequate' in the revised text.

3) MIMICA: Line 145 or later in section 3.1: Maybe you should state explicitly the reason why SIP processes are not directly implemented into MIMICA.

The original submission had this extensively discussed in the last section. In the revised text, we have moved this discussion to the beginning of section 3.

4) How does the SIP enhancement work in a case when the ice particle concentration at cloud base in MIMICA is higher than prescribed IN concentration? Does it still enhance the concentration? I assume such conditions to occur frequently in modeled boundary layer cloud.

At each model time-step and level the LES estimates the number of new nucleated particles = INP (using DeMott in the revised version) - existing N_{ice}. If this is negative, nucleation of new particles is assumed to not occur. This treatment can be found in widely used microphysics schemes (e.g. Morrison et al. 2005 in WRF). In the case that SIP is activated, the only difference is that: new nucleated particles = INP $\times$ SIP_{factor} - existing N_{ice} (thus if the outcome is negative, SIP does not enhance concentrations anymore). This methodology is better explained now in section 3.1 of the revised manuscript to avoid confusion.

5) Line 283: "The mean observed INP concentration is 0.006 L-1 and never exceeds 0.05 L-1". From where does these numbers come from? The conditions are really warm for heterogeneous ice nucleation, with modelled values at minimum -6.5 degrees and measured even warmer. What aerosol particles are active in such a warm temperature.

These statistics are based on all the flight data collected on 23 July 2013, between 10-11 UTC, at

various latitudes, longtitudes and altitudes. They aim to provide a more general overview and also allow for comparison with other ACCACIA cases (e.g. Lloyd et al. 2015), in which INP conditions are estimated and presented in a similar way. However, we acknowledge that this vague discussion is confusing to the readers as no reference to the thermodynamic conditions is made. This is now corrected in the revised manuscript. 0.006 L^{-1} is the mean concentration is for the whole flight, which sampled at temperatures between ~ -10 ^{o}C – 0 ^{o}C and specific humidity ~ 2.5–5 g m^{-3}. The maximum INP concentration is observed at ~ T= -10 ^{o}C and Qv=2.5 g m^{-3}. However the maximum ICNC occurs at T~-5^{o}C, much warmer conditions than those that maximum INPs are measured. Hence, measurements strongly indicate the occurrence of SIP.

Demott aerosol-aware parameterization predicts INP=0.03 L^{-1} around -6.5^{o}C (the coldest simulated temperatures), which interestingly is in very good agreement with the upper limit of INPs measured in the Arctic (Figure 1 above). We don't know the chemical composition of ice nuclei at these temperatures, however Wex et al. (2019) measured all types of aerosols, including bioaerosols.

6) Within MIMICA it would be possible to track temperature dependent IN concentration. How would this more realistic approach change the simulations? In comparison to observations it would have been interesting to see if the spread in modelled data is as wide as in observations. When I look at modelled data, I am really surprised how small standard deviation there is in the output. Enhancement should depend quite strongly on the updraft at the cloud base based on Figures 4, 6 and 8.

The DeMott aerosol-aware temperature-dependent parameterization is now implemented in the LES, with mean observed aerosol concentrations as input. However, the original scheme predicts INP=0.03 L^{-1} around -6.5^{o}C: even if this very low INP concentration is likely realistic (Figure 1 above), when prescribed in the LES simulations, it does not produce any ice. For this reason we have to consider the uncertainty in DeMott parameterization which is a factor of 10. Multiplying DeMott×10 yields very large INP concentrations (~0.3 L^{-1}) near cloud top (minimum -6.5^{o}C), which is unrealistic for warm subzero temperatures (Figure 1 above). For this reason, in our CNTRL simulation we apply DeMott×5. The original DeMott scheme, DeMott×10 and DeMott×100 are presented as sensitivity tests.

Below we show the mean profiles produced by the LES after spin-up period (no SIP is activated): DeMott×5 predicts concentrations (N_{ice}) varying from 0.007 L^{-1} at cloud base (~ -3^{o}C) to 0.11 L^{-1} near cloud top. An interesting finding is that N_{ice} profile does not match the vertical distribution of INPs predicted by the ice nucleation scheme (Figure 2). This is likely due to the effect of cloud mixing of ice crystals, as this more homogeneous profile develops within the first hour of simulation. If SIP was directly implemented in the LES, N_{ice} profiles would be used to calculate ice-ice collisions. Hence we use the N_{ice} profiles as input to the LPM: a mean INP concentration of 0.007 L^{-1} is prescribed at cloud base, while as the parcel ascends the new nucleated crystals estimated with a nucleation rate based on DeMott×5 (the product of updraft velocity, an assumed lapse rate of 6 K km^{-1}, and the temperature derivative of the INP estimates) until a maximum value of 1.1 L^{-1} INPs is reached; this is the maximum N_{ice}/INP concentration produced by the LES near cloud top (Figure 2). This discussion and the Figure below have been as added to the revised Supporting Information.

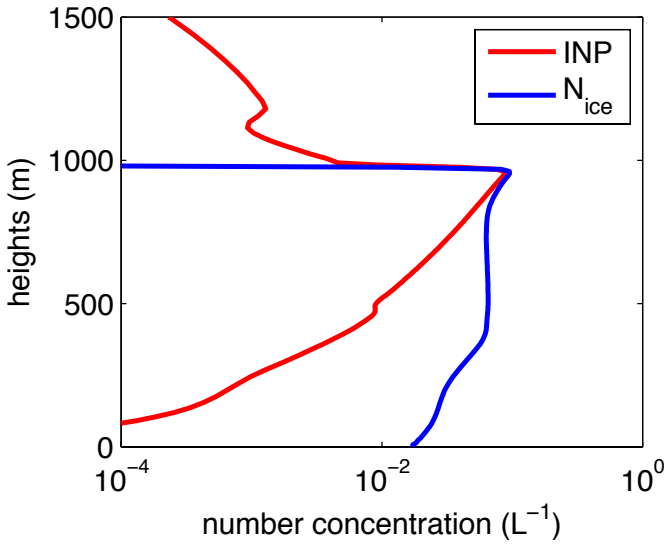

Figure 2*:* Mean LES profiles of INP and N_{ice} concentrations after spin-up period.

Furthermore, we would like to clarify that the small standard deviation in the LES simulations is not due to the prescribed INP conditions. The LES reaches a quasi-steady state after a few hours and the presented statistics are derived from that period of equilibrium. LPM is run over a relatively large parameter space, but the LES conditions are not that variable, especially in the quasi-steady state. In Figure 3a below it is obvious that only the low updraft conditions are representative of the simulated cloud (stronger updrafts are basically outliers with relative frequency < 0.2%). Also we cover in-cloud temperature conditions with the LPM; however, the parameterization in the LES is eventually a function of cloud base temperature, whose range is much narrower (Figure 3b). Since running the LPM is computational cheap, testing a larger parameter space was no problem for us: it ensures that all possible conditions are accounted for. However, now we understand that the wider thermodynamic conditions presented in Figures 4,6,8 in the previous manuscript might confuse the reader. For this reason we have moved the LPM look-up tables to the Supporting Information, while only the dominant conditions are discussed in the main text.

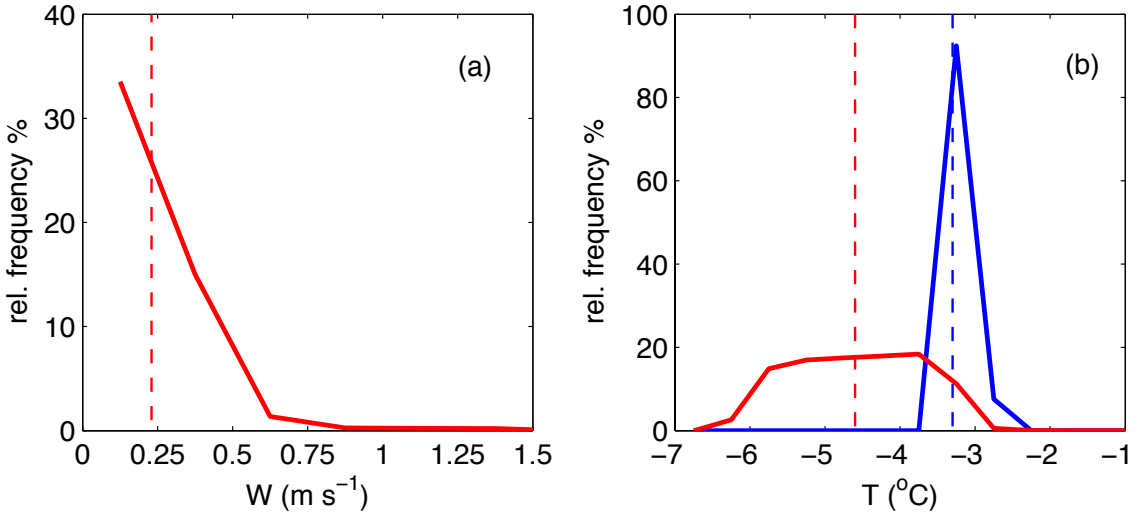

Figure 3*:* Relative frequency distribution for hourly outputs of 3D LES fields of (a) incloud updraft velocities (u_z>0.05 m s^{-1}) and (b) in-cloud (red) and cloud-base (blue) temperatures. Dashed lines represent mean values.

7) Line 463: "A main challenge in parameterizing BR is that a correct spectral representation of the ice crystals is required, which is more feasible in bin microphysics schemes". This is true, and the same limitations holds for all cases when temperature dependent ice nucleation or secondary ice production is included. If the number concentration is tuned to be correct, the size distribution and total mass is probably wrong due to given shape for size distribution.
This is a common problem in bulk microphysics schemes. The very detailed bin microphysics schemes however are computationally expensive and that's why they are not widely used in weather prediction and climate models. For this reason we suggest that LPMs can serve as a efficient way to parameterize SIP in large-scale models: although several simplifications are still employed, they likely can offer a reasonable estimate of the order of magnitude of SIP multiplication in different cloud states.

8) Jones et al., 2018 is not accepted for publication, so it should not be cited.
We have removed this citation in the revised manuscript

9) Schwarzenboeck et al., 2009 title is "Indications for stellar-crystal fragmentation in Arctic clouds"
Thank you, corrected

References:

Déry, S. J. and Yau, M. K.,1999: 'A Climatology of Adverse Winter-Type Weather Events', J. Geophys. Res. 104(D14), 16,657–16,672.

Geerts, B., B. Pokharel, and D.A. Kristovich, 2015: Blowing Snow as a Natural Glaciogenic Cloud Seeding Mechanism. *Mon. Wea. Rev.,* 143, 5017–5033,https://doi.org/10.1175/MWR-D-15-0241.1

Gossart, A., Souverijns, N., Gorodetskaya, I. V., Lhermitte, S., Lenaerts, J. T. M., Schween, J. H., Mangold, A., Laffineur, Q., and van Lipzig, N. P. M.: Blowing snow detection from ground-based ceilometers: application to East Antarctica, The Cryosphere, 11, 2755–2772, https://doi.org/10.5194/tc-11-2755-2017, 2017.

Lloyd, G., Choularton, T. W., Bower, K. N., Gallagher, M. W., Connolly, P. J., Flynn, M., Farrington, R., Crosier, J., Schlenczek, O., Fugal, J., and Henneberger, J.: The origins of ice crystals measured in mixed-phase clouds at the high-alpine site Jungfraujoch, Atmos. Chem. Phys., 15, 12953–12969, https://doi.org/10.5194/acp-15-12953-2015, 2015.

Lloyd, G., Choularton, T. W., Bower, K. N., Crosier, J., Jones, H., Dorsey, J. R., Gallagher, M. W., Connolly, P., Kirchgaessner, A. C. R., and Lachlan-Cope, T.: Observations and comparisons of cloud microphysical properties in spring and summertime Arctic stratocumulus clouds during the ACCACIA campaign, Atmos. Chem. Phys., 15, 3719-3737, https://doi.org/10.5194/acp-15-3719-2015, 2015.

Listowski, C. and Lachlan-Cope, T.: The microphysics of clouds over the Antarctic Peninsula – Part 2: modelling aspects within Polar WRF, Atmos. Chem. Phys., 17, 10195–10221, https://doi.org/10.5194/acp-17-10195-2017, 2017.

Morrison, H., Curry, J.A., & Khvorostyanov, V.I. (2005). A New Double-Moment Microphysics Parameterization for Application in Cloud and Climate Models. Part I: Description, . *Atmos. Sci.,* 62*,* 3683-3704 62

Phillips, V.T., P.J. Demott, C. Andronache, K.A. Pratt, K.A. Prather, R. Subramanian, and C. Twohy, 2013: Improvements to an Empirical Parameterization of Heterogeneous Ice Nucleation and Its Comparison with Observations. *J. Atmos. Sci.,* 70, 378–409, https://doi.org/10.1175/JAS-D-12-080.1

Pruppacher, H.R. and Klett, J.D. (1997) Microphysics of Clouds and Precipitation. 2nd Edition, Kluwer Academic, Dordrecht, 954 p.

Savre, J., and Ekman, A. M. L. (2015), Large‐eddy simulation of three mixed‐phase cloud events during ISDAC: Conditions for persistent heterogeneous ice formation. *J. Geophys. Res. Atmos.*, 120, 7699– 7725. doi: 10.1002/2014JD023006

Young, G., Jones, H. M., Choularton, T. W., Crosier, J., Bower, K. N., Gallagher, M. W., Davies, R. S., Renfrew, I. A., Elvidge, A. D., Darbyshire, E., Marenco, F., Brown, P. R. A., Ricketts, H. M. A., Connolly, P. J., Lloyd, G., Williams, P. I., Allan, J. D., Taylor, J. W., Liu, D., and Flynn, M. J.: Observed microphysical changes in Arctic mixed-phase clouds when transitioning from sea ice to open ocean, Atmos. Chem. Phys., 16, 13945–13967, https://doi.org/10.5194/acp-16-13945-2016, 2016.

Vali, G. , Leon, D. and Snider, J. R. (2012), Ground‐layer snow clouds. Q.J.R. Meteorol. Soc., 138: 1507-1525. doi:10.1002/qj.1882

The impact of Secondary Ice Production on Arctic Stratocumulus

Georgia Sotiropoulou[1], Sylvia Sullivan[2], Julien Savre[3], Gary Lloyd[4], Thomas Lachlan-Cope[5], Annica M. L. Ekman[6], Athanasios Nenes[1,7]

[1]Laboratory of Atmospheric Processes and Their Impacts, School of Architecture, Civil & Environmental Engineering, École Polytechnique Fédérale de Lausanne (EPFL), Lausanne 1015, Switzerland
[2]Department of Earth and Environmental Engineering, Columbia University, New York, 10027, USA
[3]Meteorological Institute, Faculty of Physics, Ludwig-Maximilians-University, Munich, Germany
[4]Centre for Atmospheric Science, University of Manchester, Manchester, M139P, UK
[5]British Antarctic Survey, Cambridge, CB3 0ET, UK
[6]Department of Meteorology & Bolin Center for Climate Research, Stockholm University, Stockholm, 11419, Sweden
[7]Institute of Chemical Engineering Sciences, Foundation for Research and Technology-Hellas, Patras 26504, Greece

Correspondence to: georgia.sotiropoulou@epfl.ch, athanasios.nenes@epfl.ch

Abstract. In-situ measurements of Arctic clouds frequently show that ice crystal number concentrations (ICNCs) are much higher than the number of available ice-nucleating particles (INPs), suggesting that Secondary Ice Production (SIP) may be active. Here we use a Lagrangian Parcel Model and a Large Eddy Simulation to investigate the impact of three SIP mechanisms (rime-splintering, break-up from ice-ice collisions and drop-shattering) on a summer Arctic stratocumulus case observed during the Cloud Coupling And Climate Interactions in the Arctic (ACCACIA) campaign. Primary ice alone cannot explain the observed ICNCs and drop-shattering is ineffective in the examined conditions. Only the combination of both rime-splintering (RS) and collisional break-up (BR) can explain the observed ICNCs, since both these mechanisms are weak when activated alone. In contrast to RS, BR is currently not represented in large-scale models; however our results indicate that this may also be a critical ice-multiplication mechanism. In general, a low sensitivity of the ICNCs to the assumed INP, the Cloud Condensation Nuclei (CCN) conditions and also to the choice of BR parameterization is found. Finally, we show that a simplified treatment of SIP, using a LPM constrained by a LES and/or observations, provides a realistic yet computationally efficient way to study SIP effects on clouds. This method can eventually serve as a way to parameterize SIP processes in large-scale models.

Commented [G1]: New addition

1. Introduction:

Mixed-phase clouds are a critical component of the Arctic climate system due to their warming effect on the surface radiation balance (Shupe and Intrieri, 2004; Sedlar et al., 2011) and potential impact on the melting of sea ice. These clouds are very frequent in the summer, when they occur about 80–90% of the time and can persist for days to weeks (e.g. Shupe et al., 2011). However, their representation in

mesoscale and large-scale numerical weather prediction and climate models remains elusive (Karlsson and Svensson, 2013; Barton et al., 2014; Wesslén et al., 2014; Sotiropoulou et al., 2016).

An accurate description of mixed-phase clouds in models requires a solid knowledge of the amount and distribution of both liquid water and ice (e.g., Korolev et al., 2017). Ice crystals and liquid drops form upon preexisting aerosols, termed ice nucleating particles (INP) and cloud condensation nuclei (CCN), respectively. However, the observed ice crystal number concentration (ICNC) can be orders of magnitude higher than the number of INPs (e.g., Rangno and Hobbs, 2001; Gayet et al., 2009; Schwarzenboeck et al., 2009; Lloyd et al., 2015). The enhanced ICNCs are especially surprising in the high Arctic, which is relatively clean with sparse INPs (Gayet et al., 2009; Morrison et al. 2012). Secondary Ice Processes (SIP) are suggested as the cause to explain this cloud-ice paradox (e.g., Gayet et al., 2009; Lloyd et al., 2015). SIP refers to a variety of collision-based processes that multiply the concentration of ice crystals in the absence of additional INP (e.g. Field et al., 2017, and references therein). Yet these processes are poorly represented in atmospheric models, resulting in potential errors in the representation of the surface shortwave radiation budget (Young et al., 2019).

The SIP processes known and studied to date include rime-splintering, break-up from ice-ice collisions and drop-shattering. Rime-splintering (RS) is by far the most explored of all SIP mechanisms, and refers to the production of ice splinters after super-cooled droplets rime onto small graupel (Hallett and Mossop, 1974). This process occurs effectively for temperatures between -3 and -8°C (Hallett and Mossop, 1974; Heymsfield and Mossop, 1978), when liquid droplets smaller than 13 μm and larger than 25 μm are present (Hallett and Mossop, 1974; Choularton et al., 1980). RS is the only SIP mechanism that has been extensively implemented in weather prediction (e.g. Li et al., 2008; Crawford et al., 2012; Milbrandt and Morrison, 2016) and climate models (e.g. Storelvmo et al., 2008; Gettelman et al., 2010).

Secondary ice production also occurs from collisions between ice crystals (Vardiman, 1978; Takahashi et al., 1995) that lead to their fracturing and eventual break-up (BR). This mechanism is most effective at colder temperatures than required for RS, around -15◦C (Mignani et al., 2019). There is still little quantitative understanding regarding this mechanism and its dependence on atmospheric and cloud conditions; whatever is known comes from limited laboratory experimental data (Vardiman, 1978; Takahashi et al., 1995) and small-scale modeling (e.g. Fridlind et al., 2007; Yano and Phillips, 2011; 2016; Phillips et al, 2017a,b; Sullivan et al., 2017; 2018a). Relatively few attempts have been made to incorporate this process in mesoscale models (Hoarau et al., 2018; Sullivan et al., 2018b; Fu et al., 2019).

Recent laboratory studies suggest that ice multiplication at temperatures around -15°C can also occur from shattering of droplets with diameters between 50 and 100 μm (Leisner et al., 2014; Wildeman et al., 2017; Lauber et al., 2018) with presumably at least one INP that initiates the ice

formation process. Drop-shattering (DS) has been studied with small-scale models (Lawson et al., 2015; Sullivan et al., 2018a; Phillips et al., 2018) and found to be important for a range of atmospheric conditions. Sullivan et al. (2018b) implemented parameterizations for DS and BR mechanisms in the COSMO-ART mesoscale model to study a frontal rainband, which resulted in reduced discrepancies between modeled and observed ICNCs. In contrast, Fu et al. (2019) implemented DS in the Weather and Research Forecasting (WRF) model for simulations of Arctic clouds, but found insignificant ice multiplication.

Nevertheless, the thermodynamic conditions that favor the above mechanisms can frequently occur in the Arctic. In this study, we examine the potential role of SIP during the Cloud Coupling And Climate Interactions in the Arctic (ACCACIA) flight campaign in 2013. Observations of stratocumulus clouds from the summer flights indicate that ICNCs were orders of magnitude higher than the measured aerosol concentrations that can act as INP, suggesting that ice multiplication may have taken place (Lloyd et al., 2015). To investigate this hypothesis, we use a Lagrangian Parcel Model (LPM) that includes SIP descriptions and a Large Eddy Simulation (LES) that provides a realistic representation of the boundary-layer turbulence and thermodynamic conditions.

2. ACCACIA

2.1 Measurements

The ACCACIA flight campaign took place during March, April and July 2013, in the vicinity of Svalbard, Norway. The main objectives of this campaign were to reduce uncertainties regarding microphysical processes in Arctic clouds and their dependence on aerosol properties. For this purpose, an extensive suite for microphysical and aerosol instruments was deployed (Lloyd et al., 2015; Young et al., 2016). Below, we offer a brief summary of the dataset utilized in this study.

Images of cloud particles collected with a two-dimensional Stereoscopic Probe (2D-S) at 10-μm resolution were used to calculate number concentrations and discriminate particle phase. The measured concentrations were fitted with "antishatter" tips (Korolev et al., 2011, 2013) to mitigate particle shattering on the probe and have further been corrected for shattering effects using inter-arrival time (IAT) post analysis (Crosier et al. 2013). Ice Water Content (IWC) was determined from these data, using the Brown and Francis (1995) mass dimensional relationship: IWC is the sum of the masses of all ice particles recorded by the 2D-S probe, where the mass of each particle is estimated as a function of its diameter.

A DMT Cloud Droplet Probe (CDP) measured the liquid droplet size distribution between 3-50 μm and was used to derive Liquid Water Content (LWC). A GRIMM Portable Aerosol Spectrometer

provided aerosol size distributions within the range 0.25-32 μm. Owing to a lack of direct INP measurements, GRIMM aerosol concentrations with diameter larger than 0.5 μm are used as input to the DeMott et al. (2010) parameterization (hereafter DM) for primary ice nucleation. Basic meteorological measurements (e.g. pressure, temperature, relative humidity with respect to ice) were also provided by Goodrich Rosemount probes.

Previous analyses of ACCACIA observations have shown that ice multiplication, associated with enhanced ICNCs, likely took place in summer, while ice production in springtime mixed-phased clouds was likely driven by primary ice nucleation (Lloyd et al., 2015). For this reason, our study focuses on a summer single-layer stratocumulus case observed on 23 July.

2.2 Case study

The data used in this study were collected on July 23, during Flight M194, when the aircraft flew on northerly and southerly headings through a single-layer stratocumulus around 15°E, between 78.2 and 82°N. On this day, a low-pressure system was centered on 85°N 150°W, while high-pressure systems were prevailing in the sampled region, with particularly high pressure over the north of Norway. Flight M194 sampled clouds in the trailing low pressure system. The aircraft sampled mostly downdrafts, ~5 m s^{-1}, when flying at ~1 km height and weak updrafts, ~2 m s^{-1}, above 2 km. Winds were usually from the west, except the southerly end of the flight track, where south-westerly winds were measured.

In this study, we focus on a single stratocumulus deck observed between 10:00-11:00 UTC, when the aircraft was flying between 80.8-82ºN and 14.7-15.3ºE (Fig. 1). This case study is chosen as the aircraft flew at relatively low altitudes, providing detailed information about the planetary boundary layer (PBL) structure. During this period a temperature inversion was found between 0.8 km and 1.2 km altitude, about 3ºC strong (Fig. 2a). A specific humidity inversion co-existing with the temperature inversion was also observed, with a strength of 0.5 g kg^{-1} (Fig. 2b). CDP measurements further indicate the presence of a stratocumulus layer above the first 0.5 km of the atmosphere, about 450 m deep, with a cloud top residing within the temperature inversion. Such clouds that penetrate the temperature inversion layer are very frequent in the Arctic (Sedlar et al., 2012).

The cloud droplet number concentration (N_C) observed within this hour was highly variable, ranging from 0.2 to 68 cm^{-3} (Fig. 2d), while the mean profile peaks at 30 cm^{-3}. INP estimates from DM parameterization indicate a maximum concentration of 0.05 L^{-1} measured at -9ºC (above the PBL), while the mean INP value is 0.006 L^{-1} for the observed temperature (-10 – 0 ºC) and specific humidity (2.5 – 5 g m^{-3}) range. However, the mean observed ICNC for the same conditions is 1.43 L^{-1} and 17.8 L^{-1}, respectively. The maximum ICNC occurs at T~-5ºC, thus much warmer conditions than those that maximum INPs are estimated, suggesting substantial ice multiplication. Considering that the distance

between the cloud base and the surface was more than 0.5 km, while weak to moderate horizontal wind speeds prevailed, about 5.8 m s^{-1} on average in the PBL, ICNC contributions from blowing snow are unlike (Dery and Yau, 1999; Gossart et al, 2017). For this reason we focus only on secondary ice generation from in-cloud microphysical processes.

Commented [G2]: New addition

3. Models and Methods

While RS has been extensively implemented in models, BR is more challenging to parameterize as it requires a correct spectral representation of the ice crystals. This representation is more straight-forward in bin microphysics schemes (e.g. Phillips et al. 2017b), but these are computationally expensive, and thus weather forecast and climate models typically incorporate bulk microphysical representations. It is likely that a property-based ice microphysics scheme, like the Predicted Particle Properties (P3) scheme (Morrison and Milbrandt, 2015; Milbrandt and Morrison, 2016) in WRF, can support a more realistic representation of the BR process. This scheme tracks ice mixing ratio, number, mass, and rime fraction rather than number and mass in snow, graupel, and ice crystal categories, as in bulk schemes, whose thresholds can be non-physical. However, in the current version of WRF, P3 considers only two ice categories while at least three are needed for the BR description (see Section 4.2 for a discussion).

Commented [G3]: This paragraph has been moved here from the discussion section, as suggested by the reviewer

For the above reasons, we combine for our investigations a LPM specifically developed for the study of SIP (Sullivan et al., 2017; 2018a) and the MISU/MIT Cloud and Aerosol (MIMICA) LES (Savre et al., 2015), designed for the study of Arctic clouds. The LPM allows for an adequate description of the formation, growth and evolution of cloud droplets and ice particles as they interact with each other, including SIP. The LES provides a three-dimensional description of the cloud system at a high spatial and temporal resolution, which is of similar scale as the observations. The LPM – driven by the LES conditions - is used to quantify the enhancement in ICNCs due to SIP compared to primary ice formation. The ice crystal concentration in the LES (which includes only a description of primary ice) is then enhanced by the LPM result. This coupling between the LES and LPM occurs at every timestep throughout the simulation and consists a convenient way to combine the benefits of a computationally-inexpensive bin model with the high-resolution LES. A detailed description of the modeling components and the overall modeling methods and set-up are described below.

3.1 Large Eddy Simulation (LES)

The MIMICA LES (Savre et al., 2015) solves a set of non-hydrostatic prognostic equations for the conservation of momentum, ice-liquid potential temperature and total water mixing ratio with an anelastic approximation. A 4th order central finite-differences formulation determines momentum

advection and a 2nd order flux-limited version of the Lax-Wendroff scheme (Durran, 2010) is employed for scalar advection. Equations are integrated forward in time using a 2nd order Leap-Frog method and a modified Asselin filter (Williams, 2010). Sub-grid scale turbulence is parameterized using the Smagorinsky-Lilly eddy-diffusivity closure (Lilly, 1992) and surface fluxes are calculated according to Monin-Obukhov similarity theory.

Cloud microphysics are described using a two-moment approach for cloud droplets, rain and ice particles. Mass mixing ratios and number concentrations are treated prognostically for these three hydrometeor classes, whereas their size distributions are defined by generalized Gamma functions. Cloud/rain drop processes are treated following Seifert and Beheng (2001), while liquid/ice interactions are parameterized following Wang and Chang (1993). A simple parameterization for CCN activation is applied (Khvorostyanov and Curry, 2006), where the number of cloud droplets formed is a function of supersaturation and background aerosol concentration (N_{CCN}). Ice nucleation is also parameterized following DeMott et al. (2010). To account for INP loss due to activation, the newly nucleated crystals at each timestep are estimated by taking the INP number (N_{INP}) minus the number of existing ICNCs; this is a standard method applied in microphysics schemes that do not treat INPs as a prognostic variable, e.g. Morrison et al. (2005). CCN and INP concentrations are passively advected within the model domain and not depleted through droplet activation or ice nucleation processes. A detailed radiation solver (Fu and Liou, 1992) is coupled to MIMICA to account for cloud radiative properties when calculating the radiative fluxes.

Commented [G4]: New ice nucleation scheme

All simulations are performed on a 96×96×128 grid, with constant horizontal spacing $dx = dy =$ 62.5 m. The simulated domain is 6×6 km^2 horizontally and 1.77 km vertically. At the surface and in the cloud layer the vertical grid spacing is 7.5 m, while between the surface and the cloud base it changes sinusoidally, reaching a maximum spacing of 25 m. The integration time step is variable, calculated continuously to satisfy the Courant-Friedrichs-Lewy criterion for the Leap-Frog method. Lateral boundary conditions are periodic, while a sponge layer in the top 500 m of the domain damps vertically propagating gravity waves spontaneously generated during the simulations. To accelerate the development of turbulent motions, the initial ice-liquid potential temperature profiles are randomly perturbed in the first 20 vertical grid levels with an amplitude not exceeding 0.0003 K.

3.2 Lagrangian Parcel Model (LPM)

The ice enhancement from SIP is estimated with an LPM with six hydrometeor classes for small, medium, large ice and liquid hydrometeors (Sullivan et al., 2017; 2018a). Although the bin microphysics is relatively coarsely resolved, it has served as a convenient framework for the study of ice multiplication, and especially the BR process (Yano and Phillips, 2011; Sullivan et al., 2018a).

The six hydrometeor number tendencies are solved with an explicit Runge-Kutta pair for delay differential equations (Bogacki and Shampine, 1989) and coupled to moist thermodynamic equations for pressure, temperature, supersaturation, liquid water and ice mixing ratios, and hydrometeor sizes; the latter are solved with a second-order Rosenbrock solver (Rosenbrock, 1963). CCN activation is represented in the same way as in the LES, while INP concentration is also constrained based on the LES results (see Text S1 and Fig. S1 in Supporting Information). Each resolved hydrometeors type is represented by a characteristic size that is allowed to dynamically vary over time as a function of temperature and supersaturation. Ice hydrometeors are modeled as prolate spheroids to account for their non-sphericity as in Jensen and Harrington (2015).

The characteristic major axis or radius for the LPM bins are 5 μm, 50 μm and 200 μm for the small, medium and large ice particles (e.g. graupels), respectively, and 1 μm, 12 μm, 25 μm for small, medium and large liquid droplets. The number in these classes is denoted N_i, N_g, N_G and N_d, N_r, N_R respectively. A typical timescale for ice crystals to grow to medium sizes (τ_i) for convective clouds with updraft velocities W~ 2-3 m s^{-1} and cloud base temperature T_{cbh} = 0ºC is 7.5 minutes (Sullivan et al., 2017). However, a somewhat longer τ_i is expected (~9 min) in Arctic stratocumulus conditions with T_{cbh} = -5ºC and W~ 0.75 m s^{-1} (Sullivan et al., 2017). Although the colder T_{cbh} promotes ice crystal growth, the weaker updrafts have a pronounced opposing effect. Hence for our ACCACIA case, with mean W~0.25 m s^{-1} and mean T_{cbh}~-3.5ºC, i.e. weaker vertical motions and warmer temperatures than in the Arctic case in Sullivan et al. (2017), it is reasonable to assume an even slower τ_i ~12.5 min.

The timescale (τ_g) for medium ice particles to grow to large ones can be inferred from the measurements, since the 2D-S instrument can trace ice particles larger than 75 μm. Ice particles with diameters 400 μm or larger are found systematically and at relatively larger concentrations above 830 m (Fig. S2a), hence ~260 m above the cloud base height. The estimated time for a cloud particle with a mean updraft velocity 0.25 m s^{-1} to reach this level, ascending from the cloud base is ~17.5 min. Hence a τ_g=17.5 min is assumed in our LPM simulations, somewhat faster than the timescale adopted in Sullivan et al. (2017).

A similarly empirical determination of the fallout timescale τ_G of the large ice particles is not possible. For their idealized Arctic simulation, Sullivan et al. (2017) adapted a timescale of τ_G=12.5 min. In our simulations, we tested three timescales: 12.5 min, 17.5 min and 22.5 min. Our results showed no sensitivity to these values. The simulations with τ_G=17.5 min are presented in the main text.

The timescale τ_d for small droplets to grow to medium ones is set to 5 min, based on Sullivan et al. (2017; 2018a). The timescale τ_r for medium drops to grow to large ones is constrained based on the LES simulations. The LES produces very few rain droplets with diameters greater 25 μm; the maximum raindrop concentration never exceeds 0.15 cm^{-3} in the LES (Fig. S3a). For consistency, a relatively long

growth timescale is adapted, τ_r=55 sec, which allows for a limited number of droplets to grow to large sizes, comparable to the LES results (Fig. S3b). This set-up is in general agreement with the observation that very few droplets of diameters > 25 μm were found near cloud top over the ice-pack. The fallout time τ_R of large rain droplets in the LPM is set to 60 min, the end of the simulated time, as very limited precipitation (generally < 0.1 mm day^{-1}) is produced in the LES simulations.

Secondary ice processes in the LPM include: (a) RS, when a medium or large ice particle collides with a large droplet, (b) BR, when a medium ice hydrometeor collides with a large one and (c) DS, if a raindrop freezes. These processes are included in an ice generation function along with primary ice nucleation (denoted as *NUC* below):

$$G_{ice} = \left.\frac{dN_i}{dt}\right|_{NUC} + \left.\frac{dN_i}{dt}\right|_{RS} + \left.\frac{dN_i}{dt}\right|_{BR} + \left.\frac{dN_i}{dt}\right|_{DS}$$
$$= N_{INP} + F_{RS}\left[K_{RS_g}N_g + K_{RS_G}N_G\right] + F_{BR}K_{BR}N_gN_G + F_{DS}K_{DS}N_R$$

where K_X is the gravitational collection kernel and F_X the fragment number generated by process X (where X=RS, BR, DS; in the case of RS – we consider both RS from medium (RS_g) and large (RS_G) ice particles. Collisional kernels are described as in Sullivan et al. (2017) and are functions of the relative difference of the terminal velocity of the two colliding particles. Since the ice growth equation for medium and large ice particles has an asymptotic behavior, eventually the sizes for the two bins will converge to the same values and the collisional kernel for these two ice categories will become near-zero. For this reason, a correction in Δu has been applied following Reisner et al. (1998), which accounts for underestimation in the rate of collisions when $u_G \approx u_g$:

$$|u_G - u_g| = \sqrt{1.7(u_G - u_g)^2 - 0.3u_Gu_g}$$

This correction is extensively applied in collisions of large particles in popular microphysics scheme, e.g. Morrison et al. (2005). In our model, we apply this only when medium and large ice particle sizes become comparable and the difference between their radius is smaller than 1% of the smaller particle's radius: $r_G - r_g < 0.01 r_g$.

The fragment number generated by rime-splintering is formulated on the basis of the laboratory experiments conducted by Hallet and Mossop (1974), who found a maximum of 360 splinters per milligram of rime generated round -5ºC.

$$F_{RS} = 360\rho_w\frac{\pi}{6}(2r_R)^3$$

where ρ_w is the water density and r_R represents the radius of the large droplet. This process is fully efficient in the temperature range of -4 to -6 ºC, while its efficiency is decreased by 50% for temperatures between -8 – -6 ºC and -4 – -2 ºC, and set to 5% below the optimal zone (Ferrier, 1994).

The work of Takahashi et al. (1995) is used to describe break-up, assuming that ice

hydrometeors in the medium bin undergo fracturing:

$$F_{BR} = 280(T - 252)^{1.2} e^{-(T-252)/5}$$

However, their experimental set-up was very simplified using cm-size hailballs, while one of the two colliding hydrometeors remained fixed. In our LPM simulations the ice particles in the medium bin grow from 100 μm to mm sizes (not shown), thus using the above formula would certainly lead to overestimation of the number of fragments produced. For this reason, scaling F_{BR} by a factor of 10-100 for size differences is essential (see Section 3.4 for a discussion).

A more physically-based parameterization for BR has been recently developed by Phillips et al. (2017a), which estimates F_{BR} as a function of collisional kinetic energy and depends on the colliding particles' size and rimed fraction. This results in varying treatment of F_{BR} for different ice crystal types and ice habits. Since this parameterization requires several parameters that are not available in our LPM model (e.g ice particle type, habit and rimed fraction), for its implementation a number of assumptions have to be made. First of all, since primary ice particles grow through vapor deposition and move to the second bin, we assume that this bin represents snow. Given the relatively warm temperature range (Pruppacher and Klett, 1997) and after inspection of particle images, planar ice is likely the most representative ice habit of the ACCACIA case. A rimed fraction of 0.4 is also assumed, as lower values do not yield any SIP; F_{BR} becomes less than unity ICNCs are highly underestimated. Finally, the third LPM bin is assumed to consist of sufficiently rimed particles, thus the collision type adapted in our simulation is that of snow-graupel:

$$F_{BR} = \alpha A \left(1 - exp\left\{-\left[\frac{CK_o}{\alpha A}\right]^{\gamma}\right\}\right) \quad (9)$$

$$\text{where : } K_o = \frac{m_g m_G}{m_g + m_G}\left(u_G - u_g\right)^2,$$

$$A = 1.58 \cdot 10^7 (1 + 100\Psi^2)\left(1 + \frac{1.33 \cdot 10^{-4}}{D^{1.5}}\right),$$

$$\gamma = 0.5 - 0.25\Psi,$$

$$C = 7.08\, 10^6 \psi\ ,$$

$$\psi = 3.5 \cdot 10^{-3}\ ,$$

$$a = \pi {D_s}^2$$

where D_s is the equivalent spherical diameter of the smaller ice particle which undergoes fracturing, α is its surface area and Ψ the rimed fraction. C is the asperity-fragility coefficient and ψ is a correction term for the effects of sublimation in field observations by Vardiman et al. (1978). The above description concerns collisions of either planar crystals or snow with Ψ<0.5 and diameter 500 μm < D < 5 mm with any ice particle (crystals, snow, graupel or hail). However, Phillips et al. (2017a) suggest that this parameterization can be used for particle sizes outside the recommended range as long as the input

variables to the scheme are set to the nearest limit of the range.

Commented [G5]: New addition

Drop-shattering is described as function of a freezing probability (p_{fr}), parameterized following Paukert et al. (2017), and a shattering probability (p_{sh}) based on droplet levitation experiments conducted by Leisner et al. (2014):

$$F_{DS} = 2.5 \cdot 10^{-11}(2r_R)^4 p_{fr} p_{sh}$$

Freezing is allowed only when raindrop size exceeds 100 μm and p_{sh} is a normal distribution centered at -15ºC with a standard deviation of 10ºC.

The number balance in each class is the generation function at the current time as a source and the generation function at a time delay as the sink, along with aggregation and coalescence processes. Note that aggregation occurs between small and medium ice particles and generates new particles in the largest bin. Similarly, coalescence removes droplets from the small and medium bins and generates new ones in the large raindrop category. A schematic of all these processes is shown in Fig. 3.

Finally, the hydrometeor number tendencies are coupled to the moist thermodynamic equations to account for the changing system supersaturation and thus changes in their size. All LPM equations, except the newly-implemented parameterization by Phillips et al. (2017a), are described in detail in Sullivan et al. (2017, 2018a).

3.3 Initial and boundary conditions

The atmospheric profiles used to initialize the LES are based on in-situ observations collected between 10-11 UTC on 23 July (Fig. 2), along the flight track shown in Fig. 1. The fact that the aircraft did not sample vertically through the atmosphere, but flew across a relatively large domain (9 km × 180 km) and over variable surface conditions (Fig. 1), induces some challenges for the design of the control simulation: measurements below the cloud layer and above the temperature inversion (Fig. 2a) are collected over the ocean, whereas the cloud layer is mostly sampled over the marginal-ice zones (MIZ) and the ice-pack. However, the uncertainty arising from utilizing all these measurements to construct the initial vertical profiles (Fig. 2) is not necessarily larger than utilizing reanalysis data at a similarly coarse resolution.

Since our focus is on the cloud layer, we simulate ice-covered surface conditions in the LES. The co-existent temperature and specific humidity inversions, associated with the cloud top height, as observed in Fig. 2, are typical characteristics of the summertime Arctic PBL over sea-ice (Sedlar et al., 2011; Tjernström et al., 2012). Note that cloud characteristics can vary depending on the surface type, i.e. if it is open-water, MIZ or thicker ice: N_C and ICNC are about 40%-45% lower over open-water than over ice during the examined case (not shown), suggesting that optically-thicker clouds persisted over the latter. For this reason we only use cloud measurements collected at latitudes higher than 81.7ºN (Fig. 1) and within a 9×33 km^2 ice-covered area to evaluate the simulated cloud properties.

Commented [G6]: New addition

The wind forcing is set by specifying the geostrophic wind, constant with height, equal to the observed vertical mean value of 5.8 m s^{-1}. The surface pressure is set to 1010 hPa, linearly extrapolated from low-level pressure measurements. The surface temperature is set to 0°C and surface moisture to the saturation value, which reflect summer ice conditions. Surface albedo is set to 0.65, representative of the sea-ice melting season (Persson et al., 2002). In MIMICA, subsidence is treated as a linear function of height: $w_{LS} = -D_{LS}z$, where D_{LS} is the large-scale divergence. D_{LS} here is defined through trial and error: to avoid rapid vertical cloud displacements, we prescribe $D_{LS} = 3*10^{-6}$ s^{-1}.

A N_{CCN} concentration of 50 cm^{-3} is prescribed, based on measurements of cloud droplet concentrations over the ice-pack (Fig. 2d), while the sensitivity to this choice is further tested (see Section 3.4 and 4.3). Implementing the temperature-dependent DM parameterization in the LES, with mean observed aerosol concentrations (0.6 cm^{-3}) as input, results in the development of a purely liquid cloud layer in the LES (see Section 4.3). Given that the uncertainty in the DM parameterization is about one order of magnitude (DeMott et al., 2010), we therefore assume a baseline simulation where INP estimates are multiplied with a factor of five and we further perform sensitivity simulations by increasing this factor (see Section 3.4 and 4.3).

Initial specific humidity and pressure in the LPM are set to the values measured at the cloud base (3.1 g kg^{-1} and 980 hPa, respectively). The LPM is then run over a wide temperature and vertical velocity range to encompass the in-cloud variability encountered during the LES simulation (see Section 3.4). The maximum duration for LPM simulations is set to 60 minutes, but the simulation ends also when the parcel reaches the lowest cloud temperature observed near cloud top, -6.5°C. This condition ensures that parcels do not reach colder temperatures in the LPM than those encountered in the cloud simulated by the LES.

The ice enhancement factors, defined as N_{ice}/N_{INP}, where N_{ice} is the sum of ice number concentrations in all 3 bins, are derived from the LPM calculations at the end of the simulation time. These factors are saved in look-up tables and then used by the LES: the concentration of the nucleated ice particles in each LES column is multiplied at each model time-step by an enhancement factor, which is a function of the cloud base temperature (T_{cbh}) and the mean cloud updraft velocity (W).

3.4 Sensitivity experiments

The role of SIP during the ACCACIA case is investigated with the LES, in which the SIP effect is parameterized through look-up tables that encompass the LPM results (see Section 3.3). The LPM is run over a certain range of temperature and vertical velocities, representative of the ACCACIA conditions. These ranges are determined by the 3D fields produced by the LES. Hourly outputs of the 3D LES fields indicate that in-cloud updraft velocities vary between near-zero and ~1.4 m s^{-1} (Figure S4a), while the mean W is ~0.25 m s^{-1} and only 0.2% of simulated W values exceed 0.5 m s^{-1}. The

simulated cloud temperatures span from -6.5ºC to -1.5ºC (Figure S4a); the coldest temperatures are found just below cloud top, while the cloud base temperature varies between -4ºC and -2ºC. These results are indicative of very weak convection. To cover all LES simulated conditions, the LPM is run for T_{cbh} between -5 and -1ºC and vertical velocity, W, between 0.25 and 1.25 m s^{-1}, with a step value of 0.5ºC and 0.25 m s^{-1}, respectively, to derive the ice enhancement factors.

The CNTRL simulation corresponds to the LES experiment that accounts for all SIP processes, with BR being parameterized after Phillips et al. (2017a), as this is the only physically-based description available for this process. A simulation with no active SIP mechanism is also carried out, referred as NOSIP in the text. A comparison of these simulations is found in section 4.1.

Commented [G7]: New design of the control simulation

To further examine the sensitivity of the CNTRL results to BR formulation, three additional sensitivity tests are presented in the same section. In these simulations RS and DS are parameterized as in CNTRL, but BR is now based on the Takahashi results scaled by a factor of (a) 10, (b) 50 and (c) 100 (Fig. 4). Considering that Takahashi et al. (1995) used cm-size hailballs for their experiments, case (a) corresponds to mm-size particles undergoing fragmentation, while (b) and (c) to 500-μm and 100-μm, respectively. These LES simulations are referred as (a) SIP_T0.1, (b) SIP_T0.02 and (c) SIP_T0.01, where the number indicates the magnitude of scaling applied to Takahashi's formula.

In Section 4.2, the contribution of each SIP mechanism is examined separately. For this purpose the LPM is run with only one mechanism activated at each time and the produced look-up tables are used to conduct additional LES sensitivity tests, referred as RS and BR, to reflect the mechanism that contributes to ice multiplication. DS is found to be completely inactive in the examined thermodynamic conditions (not shown) and for this reason this process is not further discussed in the text. This behavior is consistent with previous studies that have shown that a relatively warm cloud base temperature is critical for the initiation of DS (Lawson et al., 2017; Sullivan et al., 2018a) and that the Arctic environment does not favor this process (Fu et al., 2019). In addition to the BR simulation, which employs the Phillips parameterization, the more simplified descriptions based on the scaled results by Takahashi et al. (1995) are also tested; these LES simulations are referred as BR_T0.1, BR_T0.02 and BR_T0.01 to indicate the scaling factor applied.

Commented [G8]: New sensitivity simulations

In Section 4.3 the sensitivity to the prescribed N_{CCN} concentration is investigated by testing two additional values: 10 cm^{-3} and 100 cm^{-3}. This range covers a variety of atmospheric conditions, from very pristine to cases where polluted air has been advected form the south. Note that CCN can be highly variable in the Arctic, typically spanning the range 10-300 cm^{-3} within the PBL (Jung et al., 2018). Two different set-ups are used for these tests: (a) similar to the CNTRL simulation with all SIP mechanisms activated, including Phillips parameterization for BR, and (b) no active SIP mechanism. These LES simulations are referred to as (a) CCN10 and CCN100, and (b) CCN10_NOSIP and

CCN100_NOSIP, respectively.

Finally, in section 4.4 the sensitivity to primary ice nucleation is examined. The standard DM parameterization predicts concentrations <~0.03 L^{-1} for temperatures <~6.5ºC, which is very close to the upper limit of INP measurements in the Arctic for the given temperature range (Wex et al., 2019). However, when applied in the LES, it does not produce any cloud ice (see section 4.1). For this reason all LES simulations in sections 4.1-4.3 are conducted with DM parameterization multiplied with a factor of 5 (DM×5), while the simulation with the standard parameterization is presented as sensitivity test, referred as DM. DM×5 predicts INP concentrations between 0.07 L^{-1} at cloud base and 0.11 L^{-1} at cloud top, which is still reasonable for Arctic conditions (Wex et al., 2019). Considering however that the uncertainty in this ice nucleation scheme is a factor of 10 (DeMott et al., 2010), an additional test DM×10 is also performed; the maximum INP concentration near cloud top predicted by this simulation is 0.3 L^{-1}, which is likely an overestimation for Arctic clouds (Wex et al., 2019). Finally an extreme case, DM×100, is also tested where the predicted INPs are now of the same order as the ICNCs observed during ACCACIA. The simulations that have the same set-up as CNTRL but a different ice nucleation scheme are referred as DM, DM10 and DM100 in the text, while those that do not account for SIP are DM_NOSIP, DM10_NOSIP and DM100_NOSIP.

Commented [G9]: New sensitivity simulations

A summary of all LES experiments is offered in Table 1. All simulations are run for 8 hours; the first 4 hours are considered as spin-up period.

4 Results

4.1 The impact of SIP on cloud macrophysics and structure

Commented [G10]: Different structure of the 'results' section

The influence of SIP on Arctic stratocumulus is quantified by comparing the CNTRL and NOSIP LES simulations with ACCACIA measurements (Fig. 5). The ICNCs (N_{ice}) produced by the CNTRL simulation fluctuate between 1.2-1.5 L^{-1}, which is in good agreement with the median observed values, but somewhat underestimated compared to the mean. The modeled mean profile of mass mixing ratio (Q_{ice}) is also close to the median observed profile, but somewhat lower compared to the mean. In contrast, only including primary ice formation produces ICNCs below the observed range (Fig. 5a), while Q_{ice} profiles agree with only the lowest values observed (Fig. 5b).

The sensitivity of our results to the newly-implemented Phillips parameterization for BR is also examined in the same figure, by comparing CNTRL to LES simulations that employ the Takahashi scheme. The mean N_{ice} values in SIP_T0.1 are larger than the median and mean observations, however the modeled ICNCs can explain some of the largest values observed. SIP_T0.02 produces mean N_{ice} and Q_{ice} profiles in very good agreement with the mean observations, while SIP_T0.01 performs similarly to CNTRL. The differences/similarities between these LES experiments are also reflected in the LPM

results (Text S2, Fig. S5): for the dominant thermodynamic conditions (W<~0.5 m s^{-1} and -4ºC<T_{cbh}<-2ºC) Phillips parameterization (CNTRL) and SIP_T0.01 predicts an enhancement factor of ~20, while SIP_T0.1 and SIP_T0.02 produce a maximum enhancement of 1.5 and 2 orders of magnitudes, respectively.

An interesting finding is that all simulations that account for SIP produce ICNCs within the observed range, while NOSIP clearly underestimates observations. These results indicate that SIP can indeed explain the observed concentrations, despite the uncertainties in BR parameterization. The SIP_T0.02 simulation, which is in good agreement with mean observations, represents fragmentation of 500-mm particles, while SIP_T0.01 is more representative of 100-mm sizes. Phillips parameterization accounts for different sizes, however it is constrained for a specific collision type and specific particle properties (habit, rimed fraction, etc.). Nevertheless, in reality more than one collision type can happen simultaneously, while the habit and rimed fraction of the particles that undergo fracturing can vary. Moreover, in our LPM model each bin category is represented by a single diameter, while observations indicate a broad particle size spectra, up to 1.27 mm (Fig. S2b). Thus in reality μm and mm particles can undergo break-up simultaneously, which might explain the wide range of observed ICNCs in Fig. 5a.

4.2 The role of the underlying SIP mechanisms

Commented [G11]: New section

To quantify the contribution of each SIP mechanism, simulations that account for a single SIP mechanism are compared in Fig. 6. RS produces mean N_{ice} and Q_{ice} profiles that can explain only the lowest range of the observed concentrations. BR produces somewhat lower concentrations and mixing ratios than RS, and so does BR_T0.01, since this parameterization predicts similar enhancement factors as Phillips et al. (2017a) when implemented in the LPM (see Fig. S6). BR_T0.02 has a more pronounced multiplication effect than RS, however it still underestimates the mean and median observed profiles. BR_T0.1 is the only simulation that results in similar mean cloud properties to the observed.

The weak multiplication effect in RS, BR and B0.01 is also clearly manifested in the LPM results (Text S2, Fig. S6), which in weak updraft conditions produce enhancement factors <~5, while BR_T0.02 produces up to a 10-fold enhancement. The multiplication factor in BR_T0.1 can vary between 10-100 times for ACCACIA conditions, resulting in improved LES results (Fig. 6) compared to the previous set-ups. However, in this simulation the results of Takahashi et al. (1995) are scaled assuming mm-size particles, which is rather an upper limit for the ice particle sizes measured during the campaign (Fig. S2b).

Figures 4-5 indicate a strong ice generation feedback between RS and BR, which results in

substantially enhanced multiplication compared to the effect that each mechanism can have when acting alone. The new fragments ejected during rime-splintering contribute to more ice-ice collisions and thus further feed the BR multiplication process, which eventually becomes more efficient than RS (not shown). Since BR is parameterized assuming mm-size particles in BR_T0.1, which is the upper bound in observations (Fig. S2b), we suggest that the observed ICNCs are most likely caused by a combination of both mechanisms (Fig. 5a).

While RS has been extensively implemented in mesoscale and climate models, this is not the case with BR; however, our results indicate that this is also an important SIP mechanism. Our findings are in contrast to the results of Fu et al. (2019), who found that BR efficiency is limited in mesoscale simulations of autumnal Arctic clouds. However, apart from focusing on different thermodynamic conditions, another difference is that they performed offline calculations of the BR effect using the parameterization of Vardiman (1978). Another interesting fact is that while other studies (Yano and Phillips, 2011; 2016) have shown that BR can be highly effective at very cold temperatures (~ -15ºC), resulting even in explosive multiplication, in the examined conditions it acts as a weaker source of secondary ice, which in combination with RS can still significantly modulate the microphysical state of the cloud.

Following the formula of Yano and Phillips (2011), we estimate the BR multiplication efficiency $\hat{C} = 4C_o \tilde{a} \tau_g \tau_{G,}$ where C_o is the nucleation rate applied in the LPM and $\tilde{a} = \alpha F_{BR}$; α is the sweep-out rate (adapted from Yano and Phillips, 2011). Phillips et al. (2017a) and Takahashi et al. (1995) parameterization, scaled with a factor 50-100, predict <~5 fragments per collision in the temperature range of interest (Fig. 4), thus using the upper limit F_{BR} =5 in our calculations yields $\hat{C}$ =10.58, which is similar to the value $\hat{C}$ = 10 predicted in Phillips et al. (2017b). Thus the theory predicts an increase of the cloud ice concentration by a factor of ~10 over a time scale of about an hour; we assume that this is likely the maximum efficiency of BR process in Arctic stratocumulus, since 60 minutes is an upper cloud mixing timescale for such clouds.

Commented [G12]: New text

4.3 Sensitivity to CCN concentration

In this section, we examine the sensitivity of our results to the prescribed CCN concentration. The LES is run for two additional N_{CCN} conditions: 10 and 100 cm^{-3} (Fig. 7). The look-up tables used to parameterize SIP in these simulations are shown in Fig. S7.

Distinct differences are observed in cloud droplet concentrations in Fig. 7a, which are significantly reduced with decreasing N_{CCN} along with a slight decrease in cloud thickness. There is no clear impact on cloud droplet number concentrations when SIPs are excluded. ICNCs in Fig. 7b are similar for all simulations that do not account for SIP, while no substantial differences are observed in

Q_{ice} profiles (Figs 7c). In contrast, the CNTRL, CCN10 and CCN100 simulations, all produce clearly different results suggesting that increasing CCN concentrations enhances SIP activity. This is mainly due to the increasing efficiency of RS, as more drops are formed to initiate this process (see Text S2, Fig. S7). All simulations accounting for SIP are in better agreement with observations than those with no active SIP mechanism, suggesting that including a SIP parameterization can improve model performance for a variety of CCN conditions.

4.4 Sensitivity to INP concentration

Here we examine the sensitivity of our results to the INP concentration by conducting six additional LES simulations: DM, DM10, DM100, and DM_NOSIP, DM10_NOSIP, DM100_NOSIP (see Table 1 for details). The vertical N_C profiles exhibit no substantial difference between all simulations except DM100, where the cloud appears geometrically thinner (Fig. 8a). This is due to the substantial ice concentration produced in this simulation, which results in glaciation of the lower portion of the cloud (Fig. 8b). Ice properties, however, exhibit distinct differences among all INP sensitivity tests (Fig. 8b, c).

The standard DeMott parametrization (DM) results in ice properties in agreement with the lowest observed values. If no SIP is accounted for (DM_NOSIP), almost no ice is produced (Fig. 8b, c). DM10 is in good agreement with the median observations (Fig. 8b, c); however, if SIP is deactivated (DM10_NOSIP), the results agree only with the lowest range of measurements. For extremely high INP conditions, when primary nucleation alone (DM100_NOSIP) can produce the mean observed ICNCs, activating SIP results in mean concentrations of about 4-5 L^{-1}, while the simulated mean Q_{ice} profile is close to the observed mean.

The comparison of N_{ice} profiles between DM and DM_NOSIP simulations suggests that the enhancement due to SIP is about a factor of 50-100, while for CNTRL and NOSIP (DM×5) it is a factor of 15-20 (Fig. 8b). For DM10 and DM10_NOSIP the enhancement is also about one order of magnitude, while somewhat smaller when comparing DM100 and DM100_NOSIP (Fig. 8b). Thus in the LES simulations, SIP enhancement decreases with increasing primary nucleation. In contrast to the LES, the LPM results suggest that increasing INP concentrations result in more effective SIP (Fig. S7); this result is somewhat expected since larger concentrations of primary ice crystals would result in more frequent ice-ice collisions (Text S2, Fig. S8). However, the LES simulations indicate that processes that act as sinks for crystal concentrations, such as precipitation, become more effective with increasing N_{ice} and Q_{ice}.

All in all, these sensitivity simulations indicate that considering SIP processes in the LES results in an overall better representation of the cloud ice properties for a variety of INP conditions. Note that

the uncertainty in the DM parameterization is about a factor of 10 (DeMott et al., 2010) and simulations that predict primary ice within this uncertainty range are in better agreement with the observations when SIP is active. It is interesting to note that even the unrealistic case of DM100 still produces results within the observed N_{ice} and Q_{ice} range, suggesting that a SIP parameterization does not degrade model performance even when unrealistically high INP conditions are prescribed.

5. Discussion and conclusions

Semi-idealized simulations of Arctic stratocumulus clouds observed during the ACCACIA campaign are performed to investigate the impact of SIP using a LES and a LPM: the LES provides a realistic representation of the atmospheric thermodynamics, while the LPM provides a more simplified framework to parameterize SIP. The effect of three SIP mechanisms, rime-splintering (RS), collisional break-up (BR) and drop-shattering (DS), is investigated. Furthermore, the sensitivity to the choice of the BR description is also examined, using ice fragmentation rates from Phillips et al. (2017a) and Takahashi et al. (1995); the first parameterization is more advanced, accounting for changes in collisional kinetic energy of the colliding particles, while the latter is a more simplified temperature-dependent relationship. Our simulations indicate that SIP processes are essential to reproduce the observed ICNCs, which are well above the concentrations generated by primary nucleation. A good agreement with observed values of cloud ice properties is obtained when either of the BR descriptions is employed, as long as the formula derived from Takahashi et al. (1995) is properly scaled for size and a high rimed fraction is prescribed in Phillips parameterization.

When the contribution of each mechanism is examined separately, DS is found to be ineffective, which is in good agreement with previous studies of Arctic clouds (Fu et al., 2019). Moreover, both RS and BR are weak when being the only active SIP mechanism. The limited influence of RS is due to the lack of relatively large raindrops to initiate this process. RS has also been found insufficient to explain observed ICNCs in Antarctic stratocumulus clouds in a similar temperature range (Young et al., 2019). To reproduce the observations, Young et al. (2019) had to remove the liquid thresholds from the RS parameterization that allow RS activation only when sufficiently large droplets are formed. Furthermore, they had to multiply the RS efficiency by a factor of 10. The limited efficiency of BR is due to a lack of enough primary ice crystals to initiate ice-ice collisions. Our results indicate that the combination of both RS and BR is a possible explanation for the observed ICNCs; the newly generated fragments by RS further fuel the BR process, resulting in substantial ice enhancement through the latter, compared to when only one mechanism is active. Interestingly, when only RS is accounted for, the multiplication effect has to be increased by about a factor of 10-20 to obtain a good agreement with the observed ICNCs, i.e. the same factor as that used in Young et al. (2019).

Commented [G13]: New addition

Our results here indicate that at relatively warm sub-zero temperatures and in low updraft conditions, BR is a potentially important ice production mechanism, particularly in combination in RS. BR efficiency in Arctic conditions has been also documented in observational studies of mixed-phase clouds in the past (Rangno and Hobbs, 2001; Schwarzenboeck et al., 2009). Schwarzenboeck et al. (2009) analyzed measurements collected with a Cloud Particle Imager during the ASTAR (Arctic Study of Aerosols, Clouds and Radiation) campaign and found evidence of stellar-crystal fragmentation in 55% of the samples; 18% of these cases were attributed to natural fragmentation, while for the rest 82% the possibility of artificial fragmentation (e.g. shattering on the probe) could not be excluded. Moreover, they only included stellar-crystals with sizes $\gtrsim$ 300 μm in their analysis, suggesting that their estimate for natural crystal fragmentation frequency is likely underestimated.

Commented [G14]: New addition

Despite the potential significance of BR, very few attempts have been made to include this process in large-scale models. Hoarau et al. (2018) recently incorporated BR in Meso-NH which includes a two-moment microphysics scheme with three ice hydrometeor types: ice crystal, graupel and snow particles, whose sizes are determined by gamma distributions (as in most bulk schemes). To represent BR, they assumed a constant number of fragments generated when snow collides with graupel. However, this approach may result in significantly underestimated SIP as other type of collisions that include large ice crystals may occur (Phillips et al., 2017a). Sullivan et al. (2018b) did consider collisions between ice crystals and the other two hydrometeor types in a similar bulk scheme in COSMO-ART, using the original (unscaled) formula of Takahashi et al. (1995). However, their approach may instead result in an overestimated BR efficiency, as not all crystal sizes are suitable to fuel this process, including the very small fragments generated by BR. Nevertheless, one of the most important outcomes of this study is that the simple framework of the LPM, when it is driven ("tuned") by the LES thermodynamic fields provides ice number enhancement factors that bridge the model results with observations. This suggests that the LPM, when appropriately constrained by observations (or LES-type simulations), provides a promising approach towards parameterizing SIP in large-scale models.

Our results indicate that BR is likely a critical mechanism in Arctic stratocumulus clouds, where large drops are sparse and RS efficiency is limited. Thus a correct representation of this process in models will likely alleviate some of the model deficiencies in representing cloud ice properties and hence the shortwave radiation budget (Young et al., 2019). However, existing parameterizations are based on old laboratory datasets and simplified experimental set-ups (Vardiman, 1978; Takahashi et al., 1995). As there have been significant advances in the development of laboratory instruments suitable for BR studies through the past decades, we highlight the need for new laboratory experiments with more realistic set-ups that focus on the BR mechanism. We believe that constraining BR accurately in

models could have a significant impact on the representation of Arctic climate in large-scale models and projections for the future.

Code availability: The original LPM code can be found on https://github.com/scs2229/SIM. The LES code is available upon request.

Data availability: ACCACIA observations are available on https://data.bas.ac.uk and http://www.ceda.ac.uk.

Author contribution: GS and AN conceived and lead this study. AMLE and JS provided the LES code, while SS wrote the original LPM code. GL and TLC provided the ACCACIA observations. GS performed the LPM and LES simulations, analyzed the results, and together with AN wrote the main manuscript. AMLE, SS and JS were also involved in the scientific interpretation, discussion, and commented on the paper.

Competing interests: The authors declare that they have no conflict of interest.

Acknowledgements: We acknowledge support from Laboratory of Atmospheric Processes and Their Impacts at the Ecole Polytechnique Federale de Lausanne, Switzerland (http://lapi.epfl.ch) and the project PyroTRACH (ERC-2016-COG) funded by H2020-EU.1.1. – Excellent Science – European Research Council (ERC), project ID 726165. We are also grateful to ACCACIA scientific crew for the observational datasets used in this study.

References:

Barton, N. P., S. A. Klein, and Boyle, J. S.: On the Contribution of Longwave Radiation to Global Climate Model Biases in Arctic Lower Tropospheric Stability. J. Clim., 27, 7250-7269, doi: 10.1175/JCLI-D-14-00126.1, 2014.

Bogacki, P., and Shampine, L. F.: A 3(2) pair of Runge-Kutta formulas, Appl. Math. Letters, 2, 321–325, doi:10.1016/0893-9659(89)90079-7, 1989.

Brown, P. and Francis, P.: Improved measurements of the ice water content in cirrus using a total-water probe, J. Atmos. Ocean. Tech, 12, 410–414, 1995.

Choularton, T. W., D. J. Griggs, B. Y. Humood, and Latham, J. : Laboratory studies of riming, and its relation to ice splinter production. Quart. J. Roy. Meteor. Soc., 106, 367–374, doi:https://doi.org/10.1002/qj.49710644809, 1980.

Crawford, I., Bower, K. N., Choularton, T. W., Dearden, C., Crosier, J., Westbrook, C., Capes, G., Coe, H., Connolly, P. J., Dorsey, J. R., Gallagher, M. W., Williams, P., Trembath, J., Cui, Z., and Blyth, A.: Ice formation and development in aged, wintertime cumulus over the UK: observations and modelling, Atmos. Chem. Phys., 12, 4963-4985, https://doi.org/10.5194/acp-12-4963-2012, 2012.

Crosier, J., Choularton, T. W., Westbrook, C. D., Blyth, A. M., Bower, K. N., Connolly, P. J., Dearden, C., Gallagher, M. W., Cui, Z., and Nicol, J. C.: Microphysical properties of cold frontal rainbands, Q. J. Roy. Meteorol. Soc., 140, 1257–1268, doi:10.1002/qj.2206, 2013.

DeMott, P. J., Prenni, A. J., Liu, X., Kreidenweis, S. M., Petters, M. D., Twohy, C. H., Richardson, M. S., Eidhammer, T., and Rogers, D. C.: Predicting global atmospheric ice nuclei distributions and their impacts on climate, Proc. Nat. Acad. Sci., doi:10.1073/pnas.0910818107, 2010.

Durran, D.R.: Numerical Methods for Fluid Dynamics, Texts Appl. Math., 2nd ed., Springer, Berlin-Heidelberg, Germany, 2010

Ferrier, B.S.: A Double-Moment Multiple-Phase Four-Class Bulk Ice Scheme. Part I: Description. J. Atmos. Sci. , 51, 249–280, https://doi.org/10.1175/1520-0469(1994)051<0249:ADMMPF>2.0.CO;2 , 1994

Field, P., Lawson, P., Brown, G., Lloyd, C., Westbrook, D., Moisseev, A., Miltenberger, A., Nenes, A., Blyth, A., Choularton, T., Connolly, P., Bühl, J., Crosier, J., Cui, Z., Dearden, C., DeMott, P., Flossmann, A., Heymsfield, A., Huang, Y., Kalesse, H., Kanji, Z., Korolev, A., Kirchgaessner, A., Lasher-Trapp, S., Leisner, T., McFarquhar, G., Phillips, V., Stith, J., and Sullivan, S.: Chapter 7: Secondary ice production - current state of the science and recommendations for the future, Meteor. Monogr., doi:10.1175/AMSMONOGRAPHS-D-16-0014.1, 2017.

Fridlind, A. M., Ackerman, A. S., McFarquhar, G., Zhang, G., Poellot, M. R., DeMott, P. J., Prenni, A. J., and Heymsfield, A. J.: Ice properties of single-layer stratocumulus during the Mixed-Phase Arctic

Formatted: English (United Kingdom)

Cloud Experiment: 2. Model results., J. Geophys. Res., 112, D24202, https://doi.org/10.1029/2007JD008646, 2007.

Déry, S. J. and Yau, M. K.: A Climatology of Adverse Winter-Type Weather Events, J. Geophys. Res. 104(D14), 16,657–16,672.,1999

Fu, Q, and Liou, K.N: On the Correlated k-Distribution Method for Radiative Transfer in Nonhomogeneous Atmospheres, J. Atmos., 49(22): 2139–2156, doi: 10.1007/s00382-016-3040-8, 1992

Fu, S., Deng, X., Shupe, M.D., and Huiwen X.: A modelling study of the continuous ice formation in an autumnal Arctic mixed-phase cloud case, Atmos. Res., 228, 77-85, https://doi.org/10.1016/j.atmosres.2019.05.021, 2019

Gayet, J.-F., Treffeisen, R., Helbig, A., Bareiss, J., Matsuki, A., Herber, A., and Schwarzenboeck, A.: On the onset of the ice phase in boundary layer Arctic clouds, J. Geophys. Res., 114, D19201, doi:10.1029/2008JD011348, 2009

Gettelman, A., Liu, X., Ghan, S. J., Morrison, H., Park, S., Conley, A. J., Klein, S. A., Boyle, J., Mitchell, D. L., and F. Li, J.-L.: Global simulations of ice nucleation and ice supersaturation with an improved cloud scheme in the Community Atmosphere Model, J. Geophys. Res., 115, D18216, doi:10.1029/2009JD013797, 2010.

Gossart, A., Souverijns, N., Gorodetskaya, I. V., Lhermitte, S., Lenaerts, J. T. M., Schween, J. H., Mangold, A., Laffineur, Q., and van Lipzig, N. P. M.: Blowing snow detection from ground-based ceilometers: application to East Antarctica, The Cryosphere, 11, 2755–2772, https://doi.org/10.5194/tc-11-2755-2017, 2017.

Hallett, J. and Mossop, S. C.: Production of secondary ice particles during the riming process, Nature, 249, 26–28, doi:10.1038/249026a0, 1974.

Hoarau, T., Pinty, J.-P., and Barthe, C.: A representation of the collisional ice break-up process in the two-moment microphysics LIMA v1.0 scheme of Meso-NH, Geosci. Model Dev., 11, 4269-4289, https://doi.org/10.5194/gmd-11-4269-2018, 2018.

Heymsfield, A. J., and Mossop, S. C.: Temperature dependenceof secondary ice crystal production during soft hailgrowth by riming. Quart. J. Roy. Meteor. Soc., 110, 765–770,doi:10.1002/qj.49711046512, 1984

Jensen, A. A. and Harrington J. Y.: Modeling ice crystal aspect ratio evolution during riming: A single-particle growth model. J. Atm. Sci., 72, 2569-2590, doi: 10.1175/JAS-D-14-0297.1, 2015.

Jung, C.H., Yoon, Y.J., Kang, H.J., Gim, Y., Lee, B.Y., Ström, J., Krejci, R. and Tunved, P.: The seasonal characteristics of cloud condensation nuclei (CCN) in the arctic lower troposphere, Tellus B: Chemical and Physical Meteorology ,70:1, 1-13, DOI: 10.1080/16000889.2018.1513291, 2018.

Karlsson, J., and Svensson, G. Consequences of poor representation of Arctic sea-ice albedo and cloud-radiation interactions in the CMIP5 model ensemble, Geophys. Res. Lett., 40, 4374–4379, doi:10.1002/grl.50768, 2013.

Korolev, A., McFarquhar, G., Field, P.R., Franklin, C., Lawson, P., Wang, Z., Williams, E., Abel, S.J., Axisa, D., Borrmann, S., Crosier, J., Fugal, J., Krämer, M., Lohmann, U., Schlenczek, O., Schnaiter, M., and Wendisch, M.: Mixed-Phase Clouds: Progress and Challenges. Meteorological Monographs, 58, 5.1–5.50, https://doi.org/10.1175/AMSMONOGRAPHS-D-17-0001.1, 2017.

Korolev, A. V., Emery, E. F., Strapp, J.W., Cober, S. G., Isaac, G. A., Wasey, M., and Marcotte, D.: Small ice particles in tropospheric clouds: fact or artifact?, B. Am. Meteorol. Soc., 92, 967–973, doi:10.1175/2010BAMS3141.1, 2011.

Korolev, A. V., Emergy, E., and Creelman, K.: Modification and Tests of Particle Probe Tips to Mitigate Effects of Ice Shattering, J. Atmos. Ocean. Tech., 30, 690–708, 2013.

Lauber, A., Kiselev, A., Pander, T., Handmann, P., and Leisner, T.: Secondary ice formation during freezing of levitated droplets, J. Atmos. Sci., 75, 2815–2826, https://doi.org/10.1175/JAS-D-18-0052.1, 2018.

Lawson, R. P.,Woods, S., and Morrison, H.: The microphysics of ice and precipitation development in tropical cumulus clouds, J. Atm. Sci.,72, 2429–2445, doi:10.1175/JAS-D-14-0274.1, 2015.

Lawson, P., Gurganus, C., Woods, S., and Bruintjes, R.: Aircraft observations of cumulus microphysics

ranging from the tropics to midlatitudes: implications for a “new” secondary ice process, J. Atmos. Sci., 74, 2899–2920, https://doi.org/10.1175/JAS-D-17-0033.1, 2017.

Leisner, T., Pander, T., Handmann, P., and Kiselev, A.: Secondary ice processes upon heterogeneous freezing of cloud droplets, 14th Conf. on Cloud Physics and Atmospheric Radiation, Amer. Meteor. Soc, Boston, MA, 2014.

Li, G., Wang, Y., and Zhang, R.:Implementation of a two-moment bulk microphysics scheme to the WRF model to investigate aerosol - cloud interaction, J. Geophys. Res., 113, D15211, doi:10.1029/2007JD009361, 2008.

Lilly, D.K.: A proposed modification to the Germano subgrid-scale closure method, Phys. Fluids, 4: 633–635, doi:10.1063/1.858280, 1992.

Lloyd, G., Choularton, T. W., Bower, K. N., Gallagher, M. W., Connolly, P. J., Flynn, M., Farrington, R., Crosier, J., Schlenczek, O., Fugal, J., and Henneberger, J.: The origins of ice crystals measured in mixed-phase clouds at the high-alpine site Jungfraujoch, Atmos. Chem. Phys., 15, 12953–12969, https://doi.org/10.5194/acp-15-12953-2015, 2015.

Mignani, C., Creamean, J. M., Zimmermann, L., Alewell, C., and Conen, F.: New type of evidence for secondary ice formation at around −15 °C in mixed-phase clouds, Atmos. Chem. Phys., 19, 877-886, https://doi.org/10.5194/acp-19-877-2019, 2019.

Milbrandt, J.A. and Morrison, H.: Parameterization of Cloud Microphysics Based on the Prediction of Bulk Ice Particle Properties. Part III: Introduction of Multiple Free Categories. J. Atmos. Sci., 73, 975–995, https://doi.org/10.1175/JAS-D-15-0204.1, 2016.

Mossop, S. C.: Production of secondary ice particles during the growth of graupel by riming. Q.J.R. Meteorol. Soc., 102: 45-57. doi:10.1002/qj.49710243104, 1976.

Mossop, S. C., and Hallett, J.: Ice crystal concentration in cumulus clouds: Influence of the drop spectrum. Science, 186, 632–634. https://doi.org/10.1126/science.186.4164.632, 1974.

Morrison, H. and Milbrandt, J.A.: Parameterization of Cloud Microphysics Based on the Prediction of Bulk Ice Particle Properties. Part I: Scheme Description and Idealized Tests. J. Atmos. Sci., 72, 287–311, https://doi.org/10.1175/JAS-D-14-0065.1, 2015.

Morrison, H., Curry, J.A., and Khvorostyanov, V.I.: A New Double-Moment Microphysics Parameterization for Application in Cloud and Climate Models. Part I: Description, . *Atmos. Sci.,* 62*,* 3683-3704 62, 2005

Paukert, M., Hoose, C., and Simmel, M.: Redistribution of ice nuclei between cloud and rain droplets: parameterization and application to deep convective clouds, J. Adv. Model. Earth Sy., 9, 514–535, https://doi.org/10.1002/2016MS000841, 2017.

Persson, P.O.G, Fairall, C.W., Andreas, E.L., Guest, P.S., and Perovich, D.K: Measurements near the atmospheric surface flux group tower at SHEBA: Near-surface conditions and surface energy budget, J. Geophys. Res., 107(C10): 8045, doi:10.1029/2000JC000705, 2002.

Phillips, V. T. J., Yano, J.-I., and Khain, A.: Ice multiplication by breakup in ice-ice collisions. Part I: Theoretical formulation, J. Atmos. Sci., 74, 1705–1719, https://doi.org/10.1175/JAS-D-16-0224.1, 2017a.

Phillips, V.T., Yano, , J.-I., Formenton, M., Ilotoviz, E., Kanawade, V., Kudzotsa, I., Sun, J., Bansemer, A., Detwiler, A.G., Khain, A., and Tessendorf, S.A.: Ice Multiplication by Breakup in Ice–Ice Collisions. Part II: Numerical Simulations. J. Atmos. Sci., 74, 2789–2811, https://doi.org/10.1175/JAS-D-16-0223.1, 2017b.

Phillips, V.T., S. Patade, J. Gutierrez, and A. Bansemer: Secondary Ice Production by Fragmentation of Freezing Drops: Formulation and Theory. *J. Atmos. Sci.,* 75, 3031–3070, https://doi.org/10.1175/JAS-D-17-0190.1, 2018.

Pruppacher, H.R. and Klett, J.D. (1997) Microphysics of Clouds and Precipitation. 2nd Edition, Kluwer Academic, Dordrecht, 954 p.

Rangno, A. L., and Hobbs, P. V.: Ice particles in stratiform clouds in the Arctic and possible mechanisms for the production of high ice concentrations, J. Geophys. Res., 106, 15,065–15,075, doi:10.1029/2000JD900286, 2001.

Rosenbrock, H. H.: Some general implicit processes for the numerical solution of differential equations, The Comp. Jour., 5(4), 329–330, doi:10.1093/comjnl/5.4.329,1963.

Savre, J, Ekman, AML, and Svensson, G.: Technical note: Introduction to MIMICA, a large-eddy simulation solver for cloudy planetary boundary layers, J. Adv. Model. Earth Syst., 6, doi:10.1002/2013MS000292, 2015.

Schwarzenboeck, A., Shcherbakov,V., Lefevre, R., Gayet, J.-F., Duroure, C., and Pointin, Y.: Indications for stellar-crystal fragmentation in Arctic clouds, Atmos. Res.,92, 220–228, doi:10.1016/j.atmosres.2008.10.002, 2009.

Sedlar, J., Tjernström, M., Mauritsen, T., Shupe, M. D., Brooks, I. M., Persson, P. O. G., Birch, C. E., Leck, C., Sirevaag, A., and Nicolaus, M.: A transitioning Arctic surface energy budget: the impacts of solar zenith angle, surface albedo and cloud radiative forcing, Clim. Dynam., 37, 1643–1660, doi:10.1007/s00382-010-0937-5, 2011.

Seifert, A., and Beheng. K. D: A double-moment parameterization for simulating auto conversion, accretion and self collection, Atmos. Res., 59–60: 265–281, doi:10.1016/S0169-8095(01)00126-0, 2001.

Shupe, M. D. and Intrieri, J. M.: Cloud radiative forcing of the Arcticv surface: The influence of cloud properties, surface albedo, and solar zenith angle, J. Climate, 17, 616–628, doi:10.1175/1520-0442(2004)017<0616:CRFOTA>2.0.CO;2, 2004.

Shupe, M. D., Walden, V. P., Eloranta, E., Uttal, T., Campbell, J. R., Starkweather, S. M., and Shiobara, M.: Clouds at Arctic Atmospheric Observatories, Part I: Occurrence and macrophysical properties, J. Appl. Meteor. Clim., 50, 626–644, doi:10.1175/2010JAMC2467.1, 2011.

Sotiropoulou, G., Sedlar, J., Forbes, R., and Tjernström, M.: Summer Arctic clouds in the ECMWF forecast model: an evaluation of cloud parametrization schemes. Quart. J. Roy. Meteorol. Soc., 142, 387–400, doi: 0.1002/qj.2658, 2016.

Storelvmo, T., Kristjánsson, J.E., and Lohmann, U.: Aerosol Influence on Mixed-Phase Clouds in CAM-Oslo. J. Atmos. Sci., 65, 3214–3230, https://doi.org/10.1175/2008JAS2430.1, 2008.

Sullivan, S., Hoose, C., and Nenes, A.: Investigating the contribution of secondary production to ice crystal number concentrations, J. Geophys. Res., doi:10.1002/2017JD026546, 2017.

Sullivan, S. C., Kiselev, A., Leisner, T., Hoose, C., and Nenes, A.: Initiation of secondary ice production in clouds, Atmos. Chem. Phys., 18, 1593–1610, doi:10.5194/acp-18-1593-2018, 2018a.

Sullivan, S. C., Barthlott, C., Crosier, J., Zhukov, I., Nenes, A., and Hoose, C.: The effect of secondary ice production parameterization on the simulation of a cold frontal rainband, Atmos. Chem. Phys., 18, 16461–16480, https://doi.org/10.5194/acp-18-16461-2018, 2018b.

Takahashi, T., Nagao, Y., and Kushiyama, Y.: Possible high ice particle production during graupel-graupel collisions, J. Atmos. Sci., 52, 4523–4527, doi:10.1175/1520-0469, 1995.

Vardiman, L.: The generation of secondary ice particles in clouds by crystal-crystal collision, J. Atmos. Sci., 35, 2168–2180, doi:10.1175/1520-0469, 1978.

Wang, C., and J. Chang, J.: A three-dimensional numerical model of cloud dynamics, microphysics, and chemistry. 1: Concepts and formulation, J. Geophys. Res., 98, 16,787–16,798, doi:10.1029/92JD01393, 1993.

Wildeman, S., Sterl, S., Sun, C., and Lohse, D.: Fast dynamics of water droplets freezing from the outside in, Phys. Rev. Lett., 118, doi:10.1103/PhysRevLett.118.084101, 2017.

Williams, P.D.: The RAW filter: An improvement to the Robert-Asselin filter in semi-implicit integrations, Mon. Weather Rev., 139: 1996–2007, doi:10.1175/2010 MWR3601.1, 2010.

Yano, J.-I. and Phillips, V. T. J.: Ice-ice collisions: an ice multiplication process in atmospheric clouds, J. Atmos. Sci., 68, 322–333, doi:10.1175/2010JAS3607.1, 2011.

Yano, J.-I., Phillips, V. T. J., and Kanawade, V.: Explosive ice multiplication by mechanical break-up in-ice-ice collisions: a dynamical system-based study, Q. J. Roy. Meteor. Soc., 142, 867–879,

https://doi.org/10.1002/qj.2687, 2015.

Young, G., Jones, H. M., Darbyshire, E., Baustian, K. J., McQuaid, J. B., Bower, K. N., Connolly, P. J., Gallagher, M. W., and Choularton, T. W.: Size-segregated compositional analysis of aerosol particles collected in the European Arctic during the ACCACIA campaign, Atmos. Chem. Phys., 16, 4063-4079, https://doi.org/10.5194/acp-16-4063-2016, 2016.

Young, G., Lachlan-Cope, T., O'Shea, S. J., Dearden, C., Listowski, C., Bower, K. N., Choularton T.W., and Gallagher M.W.: Radiative effects of secondary ice enhancement in coastal Antarctic clouds. *Geophysical Research Letters*, 46, 23122321. , https://doi.org/10.1029/2018GL080551, 2019.

Wesslén, C., M. Tjernström, D. H. Bromwich, G. de Boer, A. M. L. Ekman, L. S. Bai, and S. H. Wang, 2014: The Arctic summer atmosphere: an evaluation of reanalyses using ASCOS data. Atmos. Chem. Phys., 14, 2605-2624, doi:10.5194/acp-14-2605-2014.

Wex, H., Huang, L., Zhang, W., Hung, H., Traversi, R., Becagli, S., Sheesley, R. J., Moffett, C. E., Barrett, T. E., Bossi, R., Skov, H., Hünerbein, A., Lubitz, J., Löffler, M., Linke, O., Hartmann, M., Herenz, P., and Stratmann, F.: Annual variability of ice-nucleating particle concentrations at different Arctic locations, Atmos. Chem. Phys., 19, 5293-5311, https://doi.org/10.5194/acp-19-5293-2019, 2019.

Tables:

Table 1: Description of the LES experiments performed in this study

Commented [G15]: New sesntivity simulations

LES experiment	SIP process active	N_{CCN} concentration (cm^{-3})	INP concentration (L^{-1})
CNTRL	RS, BR (Phillips parameterization)	50	DM×5
NOSIP	none	50	DM×5
SIP_T0.1	RS, BR (Takahashi scaled with a factor of 10)	50	DM×5
SIP_T0.02	RS, BR (Takahashi /50)	50	DM×5
SIP_T0.01	RS, BR (Takahashi /100)	50	DM×5
BR	BR (Phillips)	50	DM×5
BR_T0.1	BR (Takahashi /10)	10	DM×5
BR_T0.02	BR (Takahashi /50)	50	DM×5
BR_T0.01	BR (Takahashi /100)	50	DM×5
RS	RS	50	DM×5
CCN10	RS, BR (Phillips)	10	DM×5
CCN10_NOSIP	none	10	DM×5
CCN100	RS, BR (Phillips)	100	DM×5
CCN100_NOSIP	none	100	DM×5
DM	RS, BR (Phillips)	50	DM
DM_NOSIP	none	50	DM
DM10	RS, BR (Phillips)	50	DM×10
DM10_NOSIP	none	50	DM×10
DM100	RS, BR (Phillips)	50	DM×100
DM100_NOSIP	none	50	DM×100

Figures:

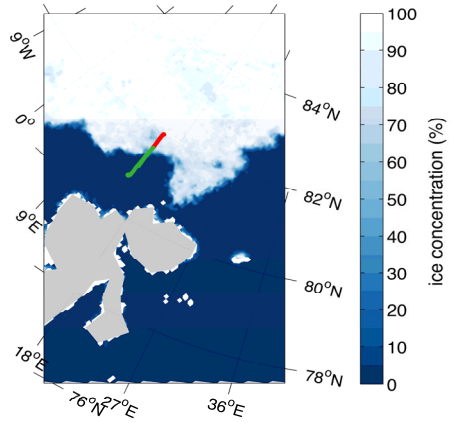

Figure 1. Advanced Microwave Scanning Radiometer (AMSR2) daily sea-ice concentrations (grid resolution 6.25 km), from University of Bremen, for 23 July 2013. Green line represents the flight track during ACCACIA campaign, between 10-11 UTC. Red line shows the flight track at latitudes > 81.7ºN; measurements collected along this track are used to evaluate the simulated cloud properties.

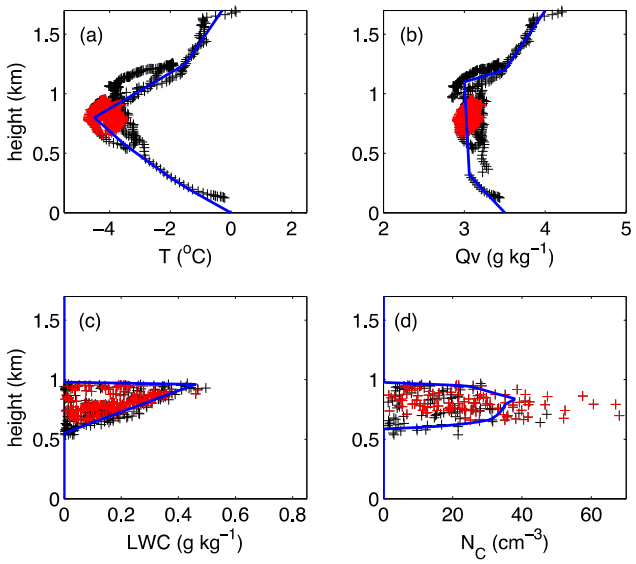

Figure 2: Measurements of (a) temperature (°C), (b) specific humidity (g kg^{-1}) and (c) liquid water content (g kg^{-1}) collected on 23 July 2013 (10-11 UTC) are indicated with black crosses. Red crosses indicate the measurements collected over the ice-pack (above 81.7°N); these are used to evaluate the simulated cloud properties. The blue lines in panels (a-c) represent the simplified vertical profiles used to initialize the LES, while in panel (d) it indicates the cloud droplet concentrations generated by the LES with CCN activation after 1 hour of simulation.

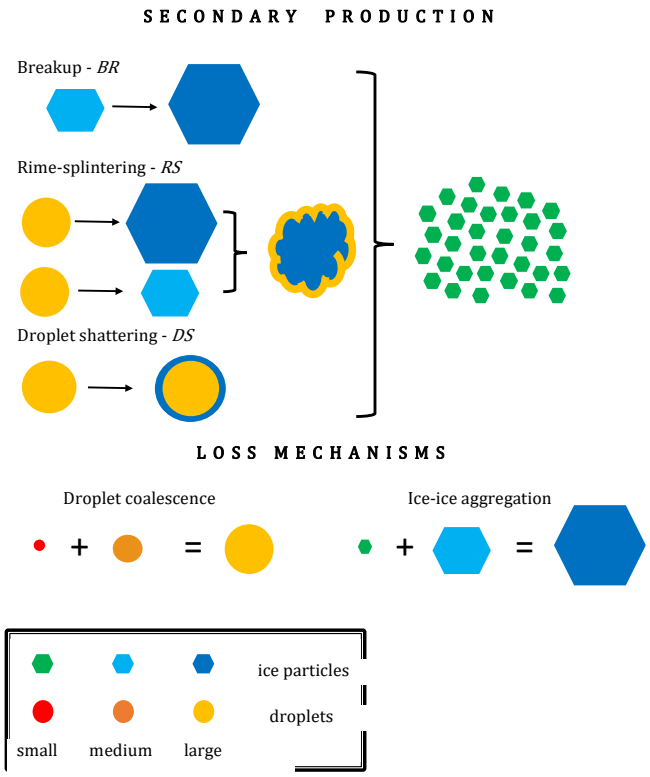

Figure 3: Schematic representation of the simplified six-bin microphysics (adopted from Sullivan et al. 2017)

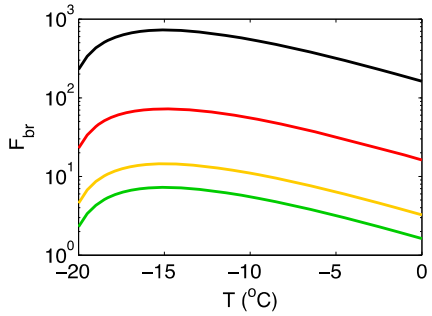

Figure 4: Number of fragments generated per collision as a function of temperature estimated with the original Takahashi's formula (black), or scaled with a factor of 10 (red), 50 (yellow) and 100 (green) to represent ice particles of mm, 500-μm, 100-μm size, respectively, that undergo fragmentation.

Commented [G16]: New figure

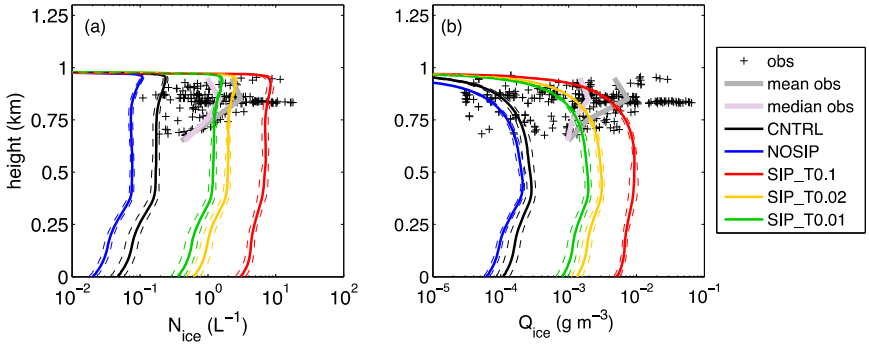

Figure 5: Vertical profiles of (a) ice crystal number concentration (N_{ice}) and (b) ice mass mixing ratio (Q_{ice}) for CNTRL (black), NOSIP (blue), SIP_T0.1 (red), SIP_T0.02 (yellow) and SIP_T0.01 (green) from the LES. Solid lines represent the mean profiles, averaged between 4-8 hours of simulation time, while dashed lines show the standard deviation. Black crosses represent the measurement range derived from the 2D-S Probe, while grey (pink) lines represent the observed mean (median) profiles.

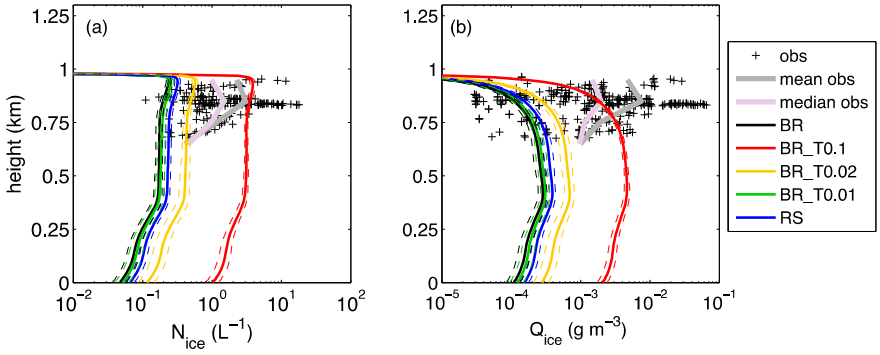

Figure 6: Same as in Fig. 5 but for the LES simulations with only one SIP mechanism active: BR (black), BR_T0.1 (red), BR_T0.02 (yellow), BR_T0.01 (green) and RS (blue).

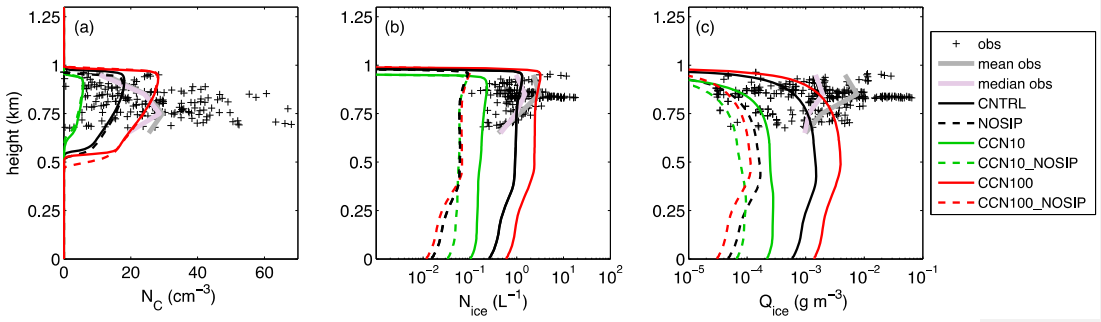

Figure 7: Vertical profiles of (a) cloud droplet concentrations (cm^{-3}), (b) ice crystal concentrations (L^{-1}) and (c) ice mass mixing ratio (g m^{-3}) for the LES sensitivity simulations with varying N_{CCN}. Black, green and red solid (dashed) lines represent CNTRL (NOSIP), CCN10 (CCN10_NOSIP) and CCN100 (CCN100_NOSIP) runs, respectively. The results are averaged between 4-8 hours of simulation time. Black crosses represent the observations, while the solid grey lines show the median observed profile.

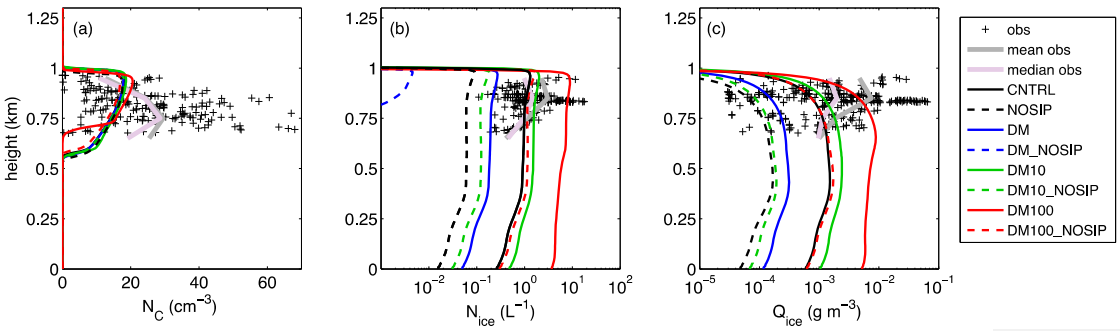

Figure 8: Same as Fig. 7 but for the LES sensitivity simulations with varying INP concentration. Black, blue, green and red solid (dashed) lines represent CNTRL (NOSIP), DM (DM_NOSIP), DM10 (DM_NOSIP), DM100 (DM100_NOSIP) experiments, respectively.